NASA TECHNICAL TRANSLATION

NASA TT F-14,044

INVESTIGATION OF FRICTIONAL PROCESSES BY MEANS OF EXOELECTRON EMISSION

Dieter Fischer

Translation of: Untersuchung von Reibungsvorgängen mit Hilfe der Exoelektronenemission", Doctoral dissertation, Berlin Technical University, Berlin, 1970, 65 pages.

N72-12414 (NASA-TT-F-14044) INVESTIGATION OF FRICTIONAL PROCESSES BY MEANS OF EXOELECTRON EMISSION Ph.D. Thesis D. Fischer (Scientific Translation Service) Nov. 1971 65 p CSCL 20K G3/15

Unclas 09382

FAC. (NASA CR OR TMX OR AD NUMBER) (CATEGORY)

NATIONAL AERONAUTICS AND SPACE ADMINISTRATION
WASHINGTON, D.C. 20546 NOVEMBER 1971

INVESTIGATION OF FRICTIONAL PROCESSES BY MEANS OF EXOELECTRON EMISSION

Dieter Fischer

ABSTRACT. Exoelectron emission was studied after aluminum, copper, and iron surfaces were activated by friction. Experiments were done with different metal combinations and at various partial pressures of oxygen, with and without water vapor. Decay curves were plotted, and glow curves were measured by heating the metals after emission decay.

Results show that exoelectron emission depends on the chemical nature and thickness of the oxide layer on the metal. The emission appears to be a power function of oxygen pressure during friction, indicating that emission can be used to measure thickness of oxide layers. Exoelectron emission is a very sensitive means of measuring transfer of one metal to another during friction when the metals are different enough to produce distinguishable emission phenomena.

1. Introduction

Many new measuring techniques and study methods have been applied in /5* recent years for the study of frictional and abrasion processes. Along with the measurement of frictional coefficients and of wear, today large modern equipment such as x-ray and electron diffraction systems, electron microscopes and microprobes are used. By means of these devices, the essential surface characteristics of metals are investigated and described.

---

*Numbers in the margin indicate the pagination in the original foreign text.

Because of their size, these devices cannot be used universally. The surface can be studied only after the friction experiment, and the atmosphere surrounding the sample must be changed. For these reasons, a study method has been sought which is as sensitive as the procedures mentioned above, and which can be used during the friction process. With this procedure, one should be able to study the effect of oxygen, i.e., the nature and thickness of the oxide layer on the samples.

One physical process, which can be observed after mechanical processing of metal surfaces and during the following oxidation, is exoelectron emission. In this work it has been applied for the first time to the study of frictional processes. It was intended to test the extent to which it is affected by the physical and chemical reactions which occur during friction experiments.

The object of the work is to determine whether the exoelectron emission effect is suitable for study of friction and wear processes, and whether an oxide coating of the metal surface can be determined by its use.

2. Summary of Previously Known Results, and Statement of the Problem /6

2.1 Friction Studies

In practice, wear is a frequent cause for machine parts wearing out and failing. When metal surfaces in machines slide over each other without enough lubrication, there is severe abrasion resulting in wear. Particles are torn out of the metal surfaces, and with large forces the parts can seize. Thus, friction is closely linked with adhesion of the two metal surfaces [1].

The form in which friction and wear appear in these processes is extremely complex, as the literature shows [2]. But in recent years most authors have accepted a classification of friction and wear processes according to four basic mechanisms. These are:

adhesive wear
abrasive wear
corrosive wear
fatigue wear

But no generally recognized definitions have yet been found for these mechanisms.

In this work we shall report essentially on the first mechanism, adhesive wear. Abrasive wear is included as a limiting case.

The large number of the friction and wear mechanisms described in the literature [2] is due essentially to the large number of parameters which directly or indirectly affect friction and wear. In many cases, there is also mutual interdependence among the parameters, so that variation of one parameter changes several others in ways which are usually uncontrollable. With this complex situation, it is understandable that generally valid results are difficult to obtain. This is also reflected in the knowledge which scientists or /7 technicians have about these processes. Most of the work available is of a purely descriptive nature. Only since 1960 have some decisive and basic works appeared (e.g., [3-5]).

In recent years, consequently, the view has prevailed that the outstanding problems can be solved only by widely applied basic research. Here, we must take into consideration the fact that the investigations will be distant from applied research.

The work presented here is intended to furnish a contribution to this basic research program. It was performed within the structure of the key-point program "Wear - Friction - Lubrication" of the German Research Society (Deutschen Forschungsgemeinschaft).

The significant parameters in friction and wear studies are:

Normal load on the sliding surfaces.

Length of the sliding path.

Temperature.

Material constants of the sliding metals.

Surface impurities.

Composition of the ambient atmosphere.

The latter two points have taken on increasing importance in recent years. The question of the ambient atmosphere plays a major role in the selection of materials for space application. The surface coating is of great importance in high temperature materials.

The effect of surface coatings, especially of oxide layers as well as their change during the process of friction, will now be described by means of some examples from the literature.

At the International Symposium on Lubrication and Wear at Houston in 1963, D. Tabor [6] reviewed frictional investigations of metals with relatively thick oxide layers. He differentiated three limiting cases.

/8

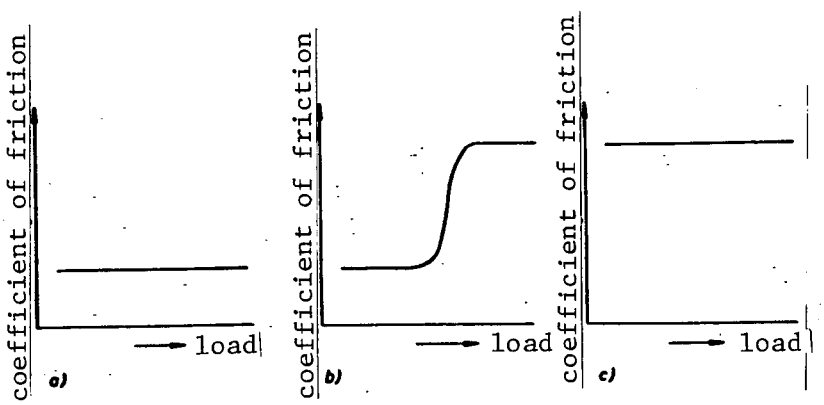

Figure 1. Effect of the mechanical properties of the oxide layer and metal on the friction process (according to Tabor [6]).

Graph (a) shows a hard oxide adhering well to a hard metal. The oxide layer is not broken through even at high loads. It acts as a separting layer between the two metals. Here metal-metal oxide friction occurs, and the coefficient of friction is small because of the absence of metallic welds.

Graph (c) shows the case of a brittle oxide film on a soft foundation. The oxide film is penetrated even at small loads, and there occurs metal-metal bridge formation and adhesive contact. The coefficient of friction is high.

Graph (b) shows the transition region between (a) and (c) with a well-adhering, not overly hard oxide on an equally hard foundation. The frictional coefficient will remain small as long as the oxide acts as a separating layer. If the oxide layer is penetrated, the coefficient of friction increases. With this model, a summary description was given, which still had to be supplemented by detailed studies. They were published, for example, by Rabinowicz [7] under the title: "Lubrication of Metals by Oxide Films". He studied sixteen metals in the temperature range from 0° C to 1600° C. With some, the coefficient of friction dropped during heating to about half the initial value. With copper, for instance, this drop occurred at 250° C; and for nickel, at 750° C. /9
Rabinowicz conjectured that the drop in the coefficient of friction was linked to the formation of a relatively soft oxide layer of definite thickness. In this respect it is important for the oxide and metal to have about the same hardness. This requirement is met by molybdenum, tantalum, copper, niobium and nickel. For lead, aluminum, and tin, the oxide is always harder than the metal, by a factor of 20, 70, and 90. A drop of the frictional coefficient as a function of temperature was not observed with these metals. These results from Rabinowicz agree well with other values [8-12]. This agreement is ascribed to the fact that all the authors used a pin-disk arrangement with a standard load of 1 kp.

Differences appeared, however, in the study of iron. Petersen, Florek, and Lee [8] found a slight drop. Kingsburg and Rabinowicz [11] ascribe the

drop to the presence of water vapor. The relationships are very complex for iron, because different iron oxides form, depending on the oxygen partial pressure and the temperature. They have a different adhesion to the base metal and different hardness, and thus very different lubricating properties. In the literature it has often been reported [9-13] that the appearance of Fe_2O_3 is linked with strong abrasive wear. Fe_3O_4 and FeO, which adhere well to α-iron, are assigned a smaller coefficient of friction.

Further interesting observations on the effect of surface oxides on frictional behavior were made by de Gee [14] and by Hensley, Male and Rowe [15] on brass alloys. De Gee observed that, in the presence of oxygen, the frictional coefficient showed a step change as a function of the zinc content of the alloy. This step change was not found in experiments under pure argon at about 7.5 atom percent zinc from $\mu = 1$ to $\mu = 8$. More accurate studies showed that below 7.5 atom percent zinc the surface was covered with a film of copper oxide which was responsible for the low coefficient of friction, as Rabinowicz [7] has shown, for example. Above 7.5 atom percent zinc, zinc oxide occurred on the surface. This result was confirmed by Hinsley, Male and Rowe, who analyzed the oxide layer on the brass surface with a microprobe. The decrease of copper content in the oxide layer could clearly be observed. /10

In the work discussed so far, the surface oxides acted as a means of separation or sliding. They decreased the coefficients of friction, as Bowden and Tabor [5] had maintained for oxide layers in general. De Gee [14] has already shown that the opposite effect can also occur. Fehling and Sarkar [16] also reported in a recent work on the opposite behavior of the same metals. Copper-nickel compounds show a poor frictional behavior if they run on each other in vacuum. Copper-nickel alloys which run on iron, in contrast, have a smaller coefficient of friction in vacuum than in air. The frictional coefficient of iron-sulfur compounds on steel has a high or a low value, depending on the nature of the surface film. The authors conjecture that, on one hand, the oxides decrease the friction if they act as a separating and lubricating

means between the metals, while, on the other hand, they increase friction if they are pressed into the surface. Which of the two effects is active depends on the hardness of the oxide.

Bellinger and de Gee [17] found an unambiguous increase in the coefficients of friction as a function of the oxygen partial pressure in the system Fe-Ag. They explained their effect by the slight solubility of the two frictional partners in each other. An explanation of this phenomenon has not yet been given. As early as 1956, Coffin [18] had reported on this effect — increase of the coefficient of friction with the formation of oxide layers on mutually insoluble metals. Since then, the problem of mutual solubility has been treated in the literature, without any unambiguous dependence having been found [19, 84].

Although the results are different with surface coatings of oxides or other layers, agreement may be expected at one point, in the absence of all surface layers. This corresponds to test conditions in ultra-high vacuum (UHV) or employment in space. Generally, there occurs a discontinuous increase in the frictional and adhesion coefficients. For many metals, one /11
observes cold-welding even with loads of the order of magnitude of a gram. But the conditions change basically again if even a monatomic layer of oxygen is absorbed. At this point, only some works by Buckley et al. may be mentioned [20-26] as representatives of many authors.

Buckley was one of the first to perform friction investigations in UHV. With his work, he contributed much to the understanding of frictional processes at different surface conditions.

But the work of Buckley shows directly that measurement of coefficients of friction and wear is no longer sufficient to obtain a generally valid statement about a wear system. Rather, it is also necessary to apply to these investigations major modern equipment such as scanning electron microscopy,

microprobe, electron and x-ray diffraction, LEED equipment (low energy electron diffraction), UHV systems, and similar research equipment, in order to exploit all the potential information.

2.2 Exoelectron Emission

Exoelectron emission is designated as an emission of electrons which occurs at or below room temperature and cannot be ascribed to ordinary phenomena such as thermionic emission, photo-effect, or radioactivity. Exoelectron emission occurs on both metals and non-metals.

Excitation is necessary to produce the emission. In most cases, this is done by mechanical working of the surface or by grinding the sample. Excitation by x-radiation or electron impact are also useful. Emission occurs even during excitation. It also continues after excitation, and decays as a function of time. Many authors [31, 32] have observed hyperbolic decay which proceeds inversely proportional to time. Decay curves have also been described, however, as superimpositions of several e-functions [37]. In the literature it is common to designate this phenomenon as post-electron emission, and the corresponding curves as decay curves. /12

But only part of the exoelectron emission is represented in the post-emission. The effect is also characterized by a capability for storage of the excited electrons. They can be released from their storage positions by the slightest energy. These energies can be provided both optically and thermally. It is sufficient, for example, to warm a mechanically worked probe slightly above room temperature, in order to re-excite emission. The upper limit of heating is usually about 400° C. In this respect, it is significant that maxima in the emission rate appear as functions of temperature during warming. These maxima are characteristic for the metal being studied, and representative of the energetic state of the storage sites. The curves recorded in this way are called, in analogy to luminescence, glow curves, the effect of thermally stimulated exoelectron emission.

As an example for exoelectron emission, the decay curve and the glow curve of a polished gold sample are shown in Figure 2. The curves indicate clearly in which form the exoelectron emission was measured.

The decay curve matches the equation for a hyperbola in the form N = constant/t (N = current density), as is demonstrated by the horizontal course of the line N·t = constant. Five hundred and ten minutes after excitation, the nearly decayed emission was newly excited by heating the sample, and a glow curve was recorded. The curve shows the characteristic maxima. The emission in this way again attains values which were measured a few minutes after working.

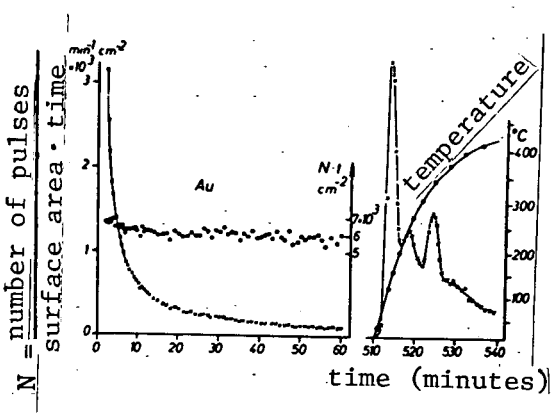

Figure 2. a) Decay with time of the exoelectron emission of a polished gold sample which was worked at time t = 0.

b) Glow curve. Beginning of heating 510 minutes after working (according to Haxel, Houtermans and Seeger [32]).

For optical stimulation, light having its wavelength far below the limit of the photoeffect was used. Ordinarily, one uses visible or long-wave ultraviolet light. Even photostimulation by infrared light has been reported (e.g., Gorlich and Ludwig [27] at a wavelength of 1,060 μm). With photostimulation one again obtains decay curves which are integrally excited. There are not yet any reliable values on spectral stimulation of the storage sites analogous to the glow curves [33, 39]. /13

Which of the two types of stimulation are applied, heating or illumination, is to be judged from the materials to be studied. Some metals such as Al and Zn respond preferentially to photostimulation, and others only to thermal emission, such as copper. There are also metals in which exoelectron emission can be demonstrated only with great difficulty. Iron is one of these.

The rules by which this selection is guided are not yet known. Experimentally, we know only that the capability for photostimulation runs parallel to the photoeffect. Thus, the alkali metals and alkaline Earth metals react most sensitively to photostimulation. /14

The analogy to luminescence mentioned above, which reappears with metals in the designation "glow curve", is of great importance for the non-metals. The phenomena of luminescence and exoelectron emission are so strongly related that the theoretical principles of luminescence have been transferred to descriptions of exoelectron emission in the non-metals with good success. This luminescence theory cannot be referred back for the theoretical description of exoelectron emission in metals, because the band model has a different appearance for the metals.

There has been no lack of attempts to describe the exoelectron emission of metals as well. So far, however, no model has been found which describes all the effects which occur, satisfactorily and without contradiction.

In the following section, the most significant theoretical explanations of exoelectron emission from metal surfaces are cited and discussed. At the same time, a review is given of the current status of knowledge about exoelectron emission from metal surfaces.

At the beginning of the 1950's, Kramer [28-31] published his works on exoelectrons. He was the first to explain the effect correctly as the emission of negative particles. Thus, exoelectron emission is called the Kramer Effect in the Eastern Block countries.

Kramer explained his effect with the occurrence of an amorphous, nonmetallic layer which is excited by mechanical working of the surface. Then this layer was supposed to return spontaneously to the crystalline state, with the heat released serving for emission of electrons.

On energetic grounds, this theory cannot be correct. Also, it provides no explanation for many of the phenomena observed. There remains only the /15
name, exoelectrons, derived from the postulated exothermic reaction.

Only one year later, Kramer, Haxel, Houtermans and Seeger [32] published an extensive work. The authors defended the view that exoelectron emission was a phenomenon accompanying renewal of the oxide layer on the sample surface. The oxide layer was removed by mechanical working. Each time an oxygen atom was adsorbed by the freed surface, an electron was supposed to be emitted by the resulting heat of adsorption.

In this explanation, exoelectron emission was for the first time related to oxygen coating of the sample surface. The time course of the emissions, as proposed by the authors, is incorrect by several orders of magnitude, however. The post-emission of exoelectrons can extend for days, as with Al, for example [38]. But monoatomic layer of oxygen is formed in microseconds at normal pressure. This model does not explain the phenomena of stimulated emission.

Grunberg and Wright [33] were the next to publish a theory, in which many authors already saw a complete description of exoelectron emission. As for the non-metals, its explanation was based strongly on the theory of luminescence. They apply the band model of insulators to the oxide coating layer and so explain the effects observed. This concept is supported by the discovery of a selective maximum in the illumination curve at λ = 4,700 Å $\triangleq$ 2.6 eV. The authors explain this maximum, in analogy with the F and F' centers in alkali halide crystals, as a transition from F-centers to F'-centers in the oxide layer. Here, those oxygen vacancy sites in the oxide layer which have one electron are called the F-centers. The F'-centers, analogously, have two electrons.

By means of this theory, the known effects could be explained for the /16
first time. But it later appeared that the authors had suffered from a

measuring error in determining a selective maximum with a wavelength of λ = 4,700 Å. The maximum was also not found by other authors.

The next step in explanation of exoelectron emission was a thoery based on the diffusion of lattice defects. It was supported by Brotzen et al. [34, 35] and by Pimbley and Ku [36]. According to Brotzen, the emission mechanism goes through the following steps:

1. Lattice defects are produced in metal and oxide by plastic deformation.

2. Defect sites which are not trapped by dislocations and wells wander to the surface. In the oxide layer, the vacancy sites can transform into singularities like the F-centers.

3. Emission occurs if these centers are depleted, perhaps by interaction with superficial surface levels.

Pimbley and Ku write:

Vacancy sites are produced in the deformed layer directly under the surface. Each vacancy site makes a certain contribution to the potential energy. If a vacancy site reaches the surface by diffusion, it becomes a preferred site for adhesion and/or oxidation, by which the potential energy of the vacancy site can be set free. If the sum of the vacancy site energy and the photon energy of the irradiating light exceeds the work function, an electron is liberated.

The authors have, on the basis of the mechanisms described, developed a mathematical model [34, 37], the results of which agree with their own experiments.

To be sure, a work by Müller and Pontinen [38] contradicts this theory. They studied worked aluminum samples, and etched the surfaces away in layers.

After each etching, the emission rate was redetermined. According to the diffusion theory, the vacancy sites responsible for the emission migrate to the surface as a function of time, so that the vacancy site concentration at the surface increases and that of the underlying layers decreases. Now, for different periods of migration, if the surface is etched away by layers, the individual samples should show different count rates because of the different vacancy site concentrations. Müller and Pontinen found no notable difference. /17

In a more recent work, Ramsey [39] has made an important step in clarification of the primary process of exoelectron emission. This is the reaction which occurs during or immediately after the mechanical working of the metal surface.

Ramsey has become prominent in his works [40 - 42] through his criticism of all previously published theories. He himself defends the idea that gas adsorption on the metal surface freshly produced by working leads to a decrease in the work function. His ideas and experiments may be cited [39] and described in the following:

1. A clean metal surface is produced by working.

2. In the next step, a monoatomic layer of oxygen is chemisorbed; or, which is no doubt the same thing, a monoatomic layer of oxide is formed (Ramsey).

3. Subsequently, dipole layers form as a result of the adsorption of water molecules. These decrease the work function. At the same time, the oxide layer begins to grow. Some time after working there exist isolated regions with an oxide layer and regions with a dipole layer adjacent to each other on the surface.

4. The dipole layer, which is presumably a monoatomic layer, forms very rapidly and produces the maximum in the electron emission (Figure 3).

On the other side, the oxide layer grows, and the water molecules become embedded in the layer. The regions of diminished work function become smaller, and the emission rate falls off. /18

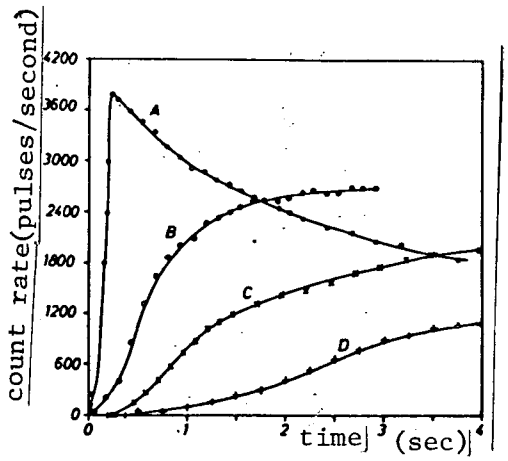

Figure 3. Count rate as a function of time after working at different air pressures.
A. 10^{-5} torr B. 2 X 10^{-6} torr
C. 10^{-6} torr D. 4 X 10^{-7} torr
(after Ramsey [39])

Ramsey has performed his experiments in UHV. With aluminum, he finds no emission at pressures below 10^{-8} torr. Scharmann and Seiber [43] could likewise measure no emission at 10^{-8} torr with aluminum. The emission begins at pressures of about 10^{-7} torr. The interesting effect now is the occurrence of an incubation time. (That is, there is a certain time after working before emission sets in.) The emission rate increases as a function of time and of the oxygen partial pressure, as Figure 3 shows.

For 10^{-7} torr the incubation time is 120 seconds. For 4 X 10^{-7} torr it is 30 seconds, and for 10^{-6} torr, 15 seconds. No incubation time is measured at 2 X 10^{-6} torr. Along with the appearance of an incubation time, it is also striking that the decay curves show a region of increase, and then drop off again (corresponding to 4). In /19 the previously known measurements, e.g., Figure 2, therefore, it has always been only the second, falling part of the curve which was detected. The time which passes before the maximum is attained is, like the incubation time, a function of the pressure. At 10^{-7} torr, 38 minutes are required; at 10^{-5} torr it is 15 seconds.

The drop in emission after attainment of the maximum is also a function of the water vapor partial pressure. Figure 4 shows the emission rate as a

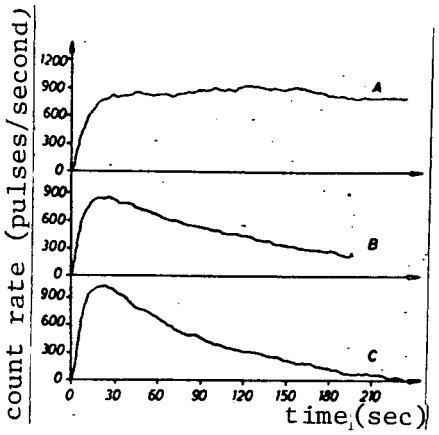

Figure 4. Count rate as a function of time after working in water vapor and oxygen

A. Water vapor 6 X 10^{-6} torr
B. Water vapor 6 X 10^{-6} torr
   Oxygen 10^{-5} torr
C. Water vapor 6 X 10^{-6} torr
   Oxygen 2.5 X 10^{-5} torr
   (after Ramsey [39])

function of time after working in a water vapor-oxygen atmosphere. Curve A was recorded in water vapor at 6 X 10^{-6} torr, and curves B and C in 6 X 10^{-6} torr water vapor with 10^{-5} torr or 2.5 X 10^{-5} torr oxygen in addition. The experiments show that the drop in emission is linked to interaction between oxygen atoms and the metal surface.

Ramsey has derived his theory /20 from the experiments described here. The incubation time is explained by the fact that the surface is being prepared for an adsorption of water. According to Huber and Kirk [44] the previous formation of a monoatomic layer of oxygen is necessary for the adsorption of water. The decrease in work function caused by adsorption of water amounts to about 1 eV, so that irradiating light with a wavelength of λ = 3450 Å can release the electrons from the metal.

In a work which has recently appeared, Linke and Meyer arrived at the same results as Ramsey. They also studied the initial stage of exoelectron emission from illuminated aluminum samples in UHV.

At this point it is of interest to draw a parallel to the friction investigations. Just as in that work by Buckley, here also the work by Ramsey through the application of UHV technology has led to new and fundamental knowledge.

But exoelectron emission has already been applied in technological investigations, independent of the still inadequate theoretical explanation.

A work of Nassenstein and Menold [45] appeared already in 1957. They find a clear relation between exoelectron emission and catalytic activity, and conjecture that the catalytic activity and the vacancy sites responsible for exoelectron emission are at least not independent of each other [46]. Recently, amplified works on exoelectron emission through catalysis and chemisorption experiments have been published. In these it is remarkable that most of these works stem from the East Bloc countries. As examples, we may mention the work of Baazov and co-workers [47, 48] on Al_2O_3 catalysts, those of Ustinova and Krylova [49-51] on ZnO and MgO catalysts, as well as those of Sato et al. on silver catalysts.

As for catalysis studies, exoelectron emission has also been strongly /21
applied in the East Bloc countries for material studies and in material testing. Here the works of Kortov and co-workers predominate [54-61]. Essentially, those authors study different steel alloys and discuss the applicability of the exoelectron emission effect in material study.

In Poland, Sujak et al. [62-73] have become prominent through extensive publications. They studied plastically deformed aluminum, as well as nickel and chromium. Fundamentally, they have conjectured an explanation of exoelectron emission. Their works led to a model which explains exoelectron emission qualitatively by micro-fractures in the oxide layer. High local field strengths occur in these micro-fractures, making possible emission in the form of field emission.

In Germany, exoelectron emission has as yet had only a little use as a study method. Hempel, Kochendörfer and Tietze [74] found no relation between the mechanical strength characteristics of aluminum and the characteristics of exoelectron emission. The preparation of the sample surface (electrolytic

polishing and/or various types of oxidation) had a very strong influence. Koch and Kuyn [75] in 1954 discussed the application of exoelectron emission for material testing. They found two regions in which the exoelectron emission procedure could be successfully applied:

1) Shaping and cutting
2) Cyclic loading

But the reproducibility of their measurements was not enough so that they could recommend immediate application of the effect. Of this work, it should be noted that the authors, like Kramer in his first works, used a peak indicator. A peak indicator has the great advantage that it can be operated in air. Thus, it can be employed anywhere, even directly in a factory. Its disadvantage is a very inaccurate indication of the incident particles, as Koch and Kuhn also observed. For this reason the peak indicator is no longer applied in exoelectron experiments since as early as the middle of the fifth decade. /22

At present, open secondary electron multipliers (SEM) serve almost exclusively for registration of the exoelectrons. These devices are sensitive, and need a good vacuum (better than 10^{-5} torr) for operation, so that material testing with exoelectrons remains limited to laboratory studies.

2.3 Statement of the Problem

In the two previous chapters, the dependence of frictional behavior and of exoelectron emission on the ambient atmosphere were discussed. The effect of oxygen was of primary importance for both processes.

In frictional processes, the surfaces sliding over each other at least partially produce a clean surface. The frictional coefficient is then determined by the adsorption starting immediately and the subsequent oxidation until renewed engagement of the surface elements.

As was shown in the previous chapter, however, the formation of an oxide layer is just the process which leads to emission of exoelectrons from metal surfaces. Both phenomena, frictional behavior and exoelectron emission, are thus decisively determined by the same physical or chemical course of reactions. This would also indicate that from the determination of one quantity, within certain limits and with well-known assumptions, one could make statements about the other quantity. This statement was tested experimentally by us.

In the present work we studied the concrete case of how exoelectron emission and frictional behavior react to the same experimental conditions. By means of the results, we shall discuss the question of whether the type /23
and degree of coating of a surface can be determined by means of exoelectron emission. A friction experiment is to serve for excitation of exoelectron emission. The result of the exoelectron experiment, that is, knowledge of the surface state of the sample, can then provide valuable indications for interpretation of the friction experiment. In certain cases, a determination of the oxide layer by means of electron diffraction is possible simultaneously with measurement of exoelectron emission.

In a second part of the work, it was to be tested whether transfer from one friction partner to another can be determined during an experiment by means of exoelectron emission. Here, of course, the friction partners must consist of different metals. The stimulus for this investigation came from a work published by Kramer in 1967 [76]. He had in the meantime extended exoelectron emission to an analytical procedure in which as little as 10^{-12} g is detectable.

3. Experimental Part /24

3.1 Design of the System

Figure 5 shows the general design of the measuring system.

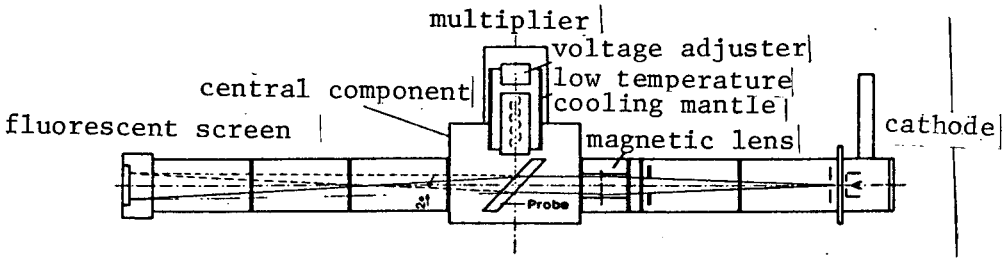

Figure 5. Design of the measuring system.

The system consists of a central component, from which the tubes of the electron diffraction apparatus extend horizontally at the sides. The friction system is placed in the central component, and the oven for heating the sample.

At the beginning of the experiment, a tensile breaking system was also used. The sample mount and the force measuring system, a continuous ring and an inductive distance pickup, are also within the central component. The tensile stress was produced with a worm drive and introduced into the central component by a draw rod. The apparatus was sealed with a tombac tube.

The secondary electron multiplier (SEM) for measurement of the exoelectrons penetrates through the cover of the central unit. The entrance opening of the SEM is 37 mm above the sample.

3.2 The Vacuum System

/25

A commercial pump assembly from the Leybold Company was used to produce the vacuum. Because of the open SEM, special precautions had to be taken to guarantee the most oil-free vacuum possible. Excessive backflow of the pump oil, and especially of the fore-pump oil, would lead to contamination of the SEM dynodes and make them useless. The oil backflow was eliminated as much as possible by the installation of an adsorption trap between the fore- and

diffusion pumps, and of low-temperature cold traps following the diffusion pump. Figure 6 shows the design of the pump stand.

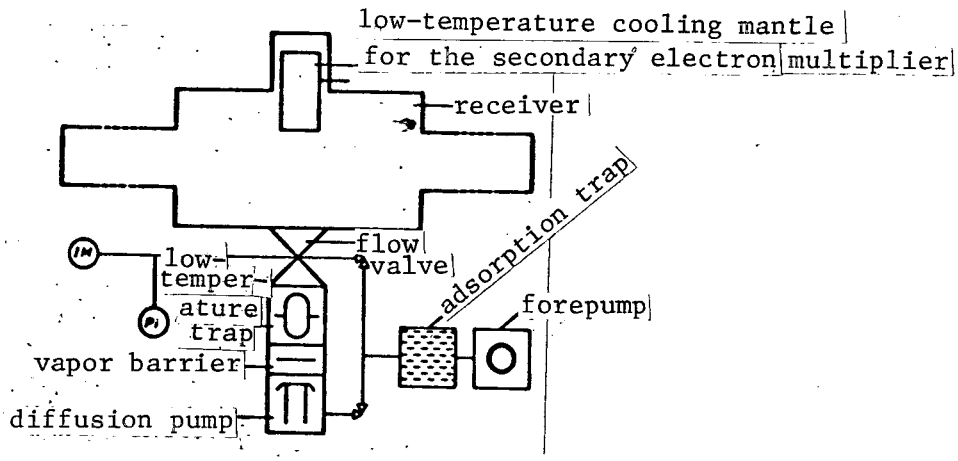

Figure 6. Vacuum system for the measuring apparatus.

The fore-vacuum was produced with a two-stage rotary vane pump. In the fore-vacuum line there was a zeolite adsorption trap which could be cooled to the temperature of liquid nitrogen if necessary. The high vacuum was produced by a three-stage oil diffusion pump (Leybodiff [170]). Above the diffusion pump there was a water-cooled vapor barrier and a low-temperature trap filled with liquid nitrogen. The filling lasted for more than 14 hours, so that sufficient cooling was guaranteed over-night. The pump assembly was closed off from the apparatus with an oil-free spring bellows valve.

A thermal conductivity manometer served for pressure measurement in the fore-vacuum region (Leybold Thermotron II), while an ionization manometer with a Bayard-Alpert tube (Leybold IM 41) served in the high-vacuum region. A mechanical manometer (1% accuracy) was used for pressure measurement in the range above 10 torr. /26

The best pressure obtained was about 5×10^{-7} torr after 24 hours pumping. Longer pumping times produced no further decrease in pressure.

The reproducibly attainable working pressure was about 1×10^{-6} torr, and the pumping time necessary for this was about one hour, if the system had not been exposed too long to the air. This pumping time could be decreased even more by employment of another cold finger (compare 3.3).

3.3 Counting System for the Exoelectrons

The exoelectrons, which leave the metal surface due to one of the mechanisms discussed in the previous section, have a mean energy of some 1.1 eV, as Scharmann and Kriegseis [77] have shown. Thus, they can be registered only with a Geiger-Müller counter, a flow-through counter, or an open SEM. Both the first detection systems require a defined atmosphere, a special gas mixture with a pressure of some 100 torr. Thus, they are unsuitable for tests in high vacuum. Thus, an open SEM was used. It has 17 stages and attains a maximum amplification of 10^7 - 10^8 at an applied high voltage of 3.6 kV. The SEM was produced by the Federal Technical University of Zurich, Division for Industrial Research. The dynodes were of Cu-Be. The SEM is only sensitive to light with wavelength below $\lambda < 3{,}300$ Å, so that it can be operated in daylight.

The entrance opening of the SEM has a size of 18×6 mm^2. Its long axis was arranged parallel to the long axis of the sample. To protect the SEM from contamination, and to decrease the background count, the SEV was placed in a /27
copper cylinder. This cylinder could be cooled by thermal conduction to the temperature of liquid nitrogen. It was always inserted into the system along with the SEM and cooled to the temperature of liquid nitrogen before high voltage was applied to the SEM (see Figure 5, page 19).

We produced the voltage divider ourselves. It has a total resistance of 8 k Ω. This corresponds to an individual resistance of 470 M Ω per dynode*. The cross current through the multiplier amounts to 0.4 mA at a voltage of

*Translator's Note: The units are obviously reversed: should be 470,000 ohms per dynode and a total resistance of 8 M-ohms (megohms).

3.4 kV. The power loss is less than 0.1 watt. Vitrified resistors were used as voltage divider resistances in order to avoid degassing in the vacuum. For the same reason, the high voltage capacitors were cast in Araldite. The high voltage and signal lines were introduced into the apparatus by glass-insulated vacuum-tight high frequency plug connectors (Amphenol BNC or HN).

At the beginning of the work, the SEM high voltage was 3 kV. By the end of the experiments it had been raised to 3.5 kV, because the amplification of the SEM decreased. It was adjusted according to the energy spectrum of a tungsten filament lamp glowing weakly red. The electrons emitted obeyed a Maxwell distribution. The high voltage was then adjusted so that the lower limit of detectable sensitivity was about half the height of the front edge. The electrons emitted were, as the exoelectrons to be measured, post-accelerated. The post-acceleration voltage exactly matched the voltage between two dynodes, about 200 V.

The count pulses from the multiplier were further processed in a Siemens Type 1 t measuring system. The system consisted of the following units: High voltage supply, linear amplifier, discriminator, mean value meter, potentiometric recorder, counter-clock unit, printer, and pulse spectroscope.

The count rate of the decay curve was recorded with the built-in potentiometric recorder. For recording the glow curve, the output of the average-value meter was input to the Y-axis of an X-Y recorder (Hewlett-Packard Moseley /28 7001 AM). The X-axis was connected directly to the thermocouple for measurement of the sample temperature. Thus, one obtains the emission rate directly as a function of the temperature. Figure 7 shows a block diagram of the system.

3.4 Arrangement for Measurement of Friction

The individual elements for measurement of coefficients of friction are described by means of the next illustration (Figure 8).

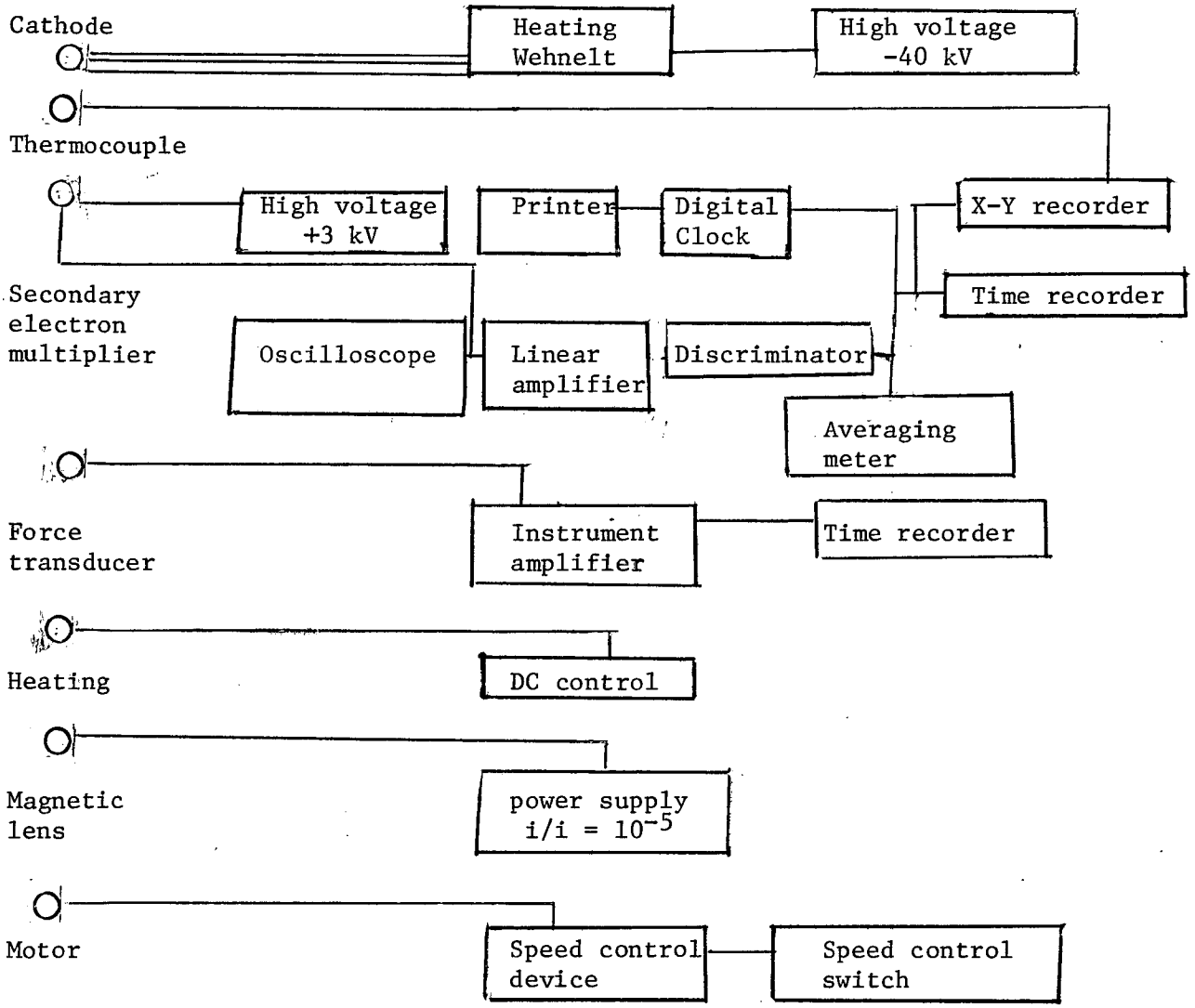

Figure 7. Block diagram of the system.

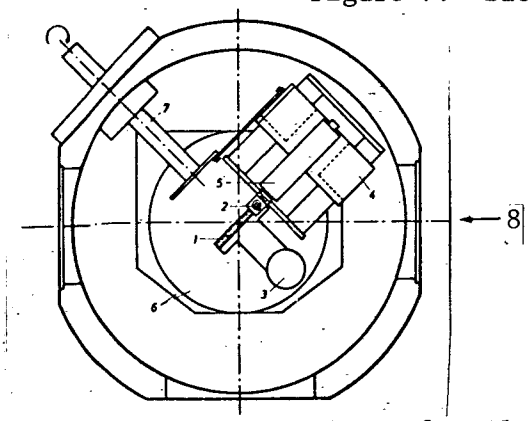

1. Comparison sample
2. Pin sample
3. Heating system
4. Sample slide
5. Force transducer
6. Sample table
7. Drive shaft
8. Electron beam

/29

Figure 8. Plan of the central component.

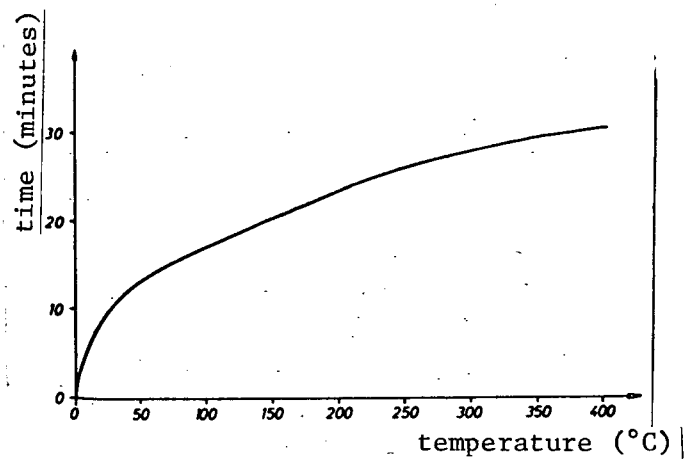

Figure 9. Heating curve of the heating system.

The metal sample is bolted to a sample holder which simultaneously makes up the heating system. The heating system consists of a soldering iron cartridge (220 W soldering coil). In place of the soldering iron point, a tongue was attached, to the front surface of which the sample is bolted. The soldering iron cartridge was operated at one-fourth its nominal power. At a higher working power, the heating wires burned out in the vacuum. Direct current was used for operation.

Figure 9 shows the heating curve for samples.

It is not linear with time, as is otherwise usual in exoelectron experiments. We did not attempt that, as it is not the goal of the work to give a quantitative analysis of the glow maxima, but first to study only qualitatively a relation between exoelectron emission and surface coating of the sample.

The pin-shaped comparison sample is guided by a slot. The slot guarantees /30 that the pin will remain in the same position in the rubbing trace. It runs in teflon bearings on two polished rods. The force pickup is mounted on the sample slot. In the course of the work, two force pickups were used. The first was of our own construction. It consisted of two unilaterally stressed leaf springs. The deflection was measured with an inductive motion pickup. From 0 to 50 p the force pickup showed a linear dependence of deflection on force.

The second force pickup (Hottinger Company Type Q 11/100) had a measuring range from 0 to 100 p. The measuring principle is identical with that of the force pickup which we built.

The sample mount for the pin sample was bolted to the pull rod of the force pickup. The pin sample stands on the comparison sample with its own weight. The pin samples were weighted with a bar to provide a definite downward pressure.

The sample slide itself is moved back and forth with a crank drive. The motor can be controlled by a device for adjusting the number of rotations. With a mechanical preselector pulse counter the number of movements of the pin over the sample can be pre-set. When the set rubbing distance is reached, the counter turns off the motor. The length of the sliding path on one back and forth motion of the pin across the sample surface is 57.2 mm. In this work the sliding path is stated in multiples of this unit, e.g., 10x, 50x, 100x.

The signals from the force pickup are picked up by a carrier frequency instrument amplifier (Hottinger Company, KWS 3S-5). Its output is recorded with a fast-writing potentiometric recorder (Linseis Company). Because of the alternating pressure and tension loading of the force pickup, the recorder produces a step-formed curve. The distance between the outer limiting lines corresponds to twice the tangential force.

3.5 The Electron Diffraction System /31

An electron diffraction system was used to investigate the sample surface. It was built horizontally, as the comparison sample was arranged horizontally in the friction experiments, in order to ensure a standard loading. No disadvantages appeared, however, other than a somewhat complicated mode of working — the diffraction image had to be viewed in a mirror. The system was built according to the ray path sketched in Figure 10.

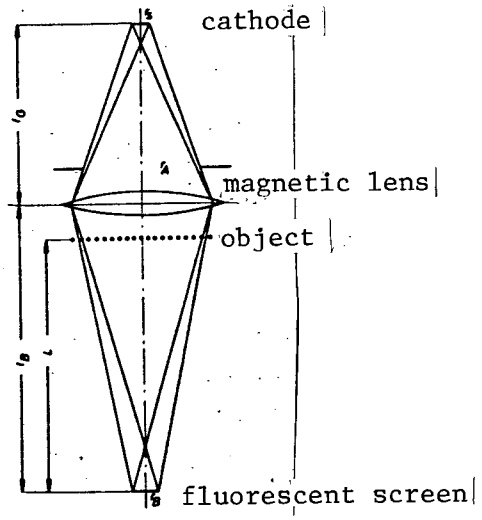

Figure 10. Beam path in the diffraction apparatus.

As appears from Figure 10, the diffraction system is designed as a single-stage system. This means that the electron source is imaged by a lens onto the recording plane. This ray path provides a high image brightness with sufficient resolution capability.

The parameters indicated have the following values: diameter of the anode diaphragm r_S = 50 μ; object distance l_G = 475 mm; image distance l_B = 735 mm; camera length L = 565 mm; diameter of the aperture diaphragm r_A = 200 μ. From these the diameter of the primary spot in the recording plane can be calculated as $r_B \sim 80$ μ.

According to Bauer [78] this value provides a resolution capability of $A = d/\Delta d$ of $A \sim 400$ for d = 1 Å. This theoretical value is completely sufficient for the reflection diffraction used here. Due to the reflection broadening which occurs as a result of the condition of the surface, the measuring inaccuracy is markedly greater than the resolving power for which we strived (see Raether [79]). /32

A cathode according to Boersch [80] served for electron production. The Wehnelt electrode was turned in the shape of a funnel with an opening angle of 90°. By carefully polishing down all the corners, operating values up to 50 kV could be attained for the cathode. The high voltage was taken from a Zeiss high voltage supply (HA 60 R) with a voltage constancy of 6×10^{-4}. The voltage supply for the Wehnelt electrode and the power supply for heating were installed in a separate housing. The potential of the Wehnelt electrode was controlled with batteries. The maximum potential was -600 V. The range from

-300 V to -600 V was controllable in 10 steps. The cathode, of thoriated tungsten wire 0.12 mm in diameter, was heated directly. The heating current was taken from a battery and controlled by preset resistances.

The electron lens used is an electromagnetic lens in an iron-enclosed design. It was computed according to early works of Ruska [81, 82] and of Picht [83]. The number of ampere-turns needed for imaging agreed with their data, at 800 - 900. In the practical design, the coil had 2,000 windings with a maximum current load of 0.5 A. The coil current was taken from a constant-current device (Heinzinger Company) with a current stability of 10^{-5}.

The magnet coil is adjustable by 5 mm in the X and Y directions in the plane perpendicular to the electron beam. The coil can also be tilted, so that the incidence angle of the electron beam on the sample can be changed. The sample table with its sample holder (see Figure 8, page 23) is likewise adjustable by some 4 mm in height. The sample table is adjusted by a reduction gear, so that the sample can be led very exactly to the beam.

Behind the sample, from the surface of which a reflection diffraction image is produced, there is a gold preparation turned into the beam. The diffraction at the gold preparation occurs in transmission. The gold preparation serves for calibration. But since it does not sit at the same position as the sample, it must still be calibrated itself. For this purpose, the surface of a sample is smoked with MgO. A diffraction picture is made of the smoked sample and the gold preparation. /33

The diffraction image is intercepted at a fluorescent screen and photographed with a miniature camera. X-ray film served as the photographic material (Agfa Gevaert Scopix G). The exposure time was between 1 second and 4 seconds.

The fluorescent material was sedimented on the glass disk after all contaminating particles and larger fluorescent particles had been filtered out of

solution. The sedimented fluorescent screen is characterized by particularly fine grain and good adhesion. After assembly, the fluorescent screen was thinly vapor-coated with gold from the inside, i.e., from the vacuum side, along with the fluorescent screen housing. The layer thickness was about 200 Å. The vapor coating made the fluorescent layer conductive, avoiding charge-up phenomena.

3.6 Materials Used

The following materials were used in the measurements: iron, copper, aluminum. The iron was obtained in rod form from the HEK company at a purity of 99.998%.

The copper samples were of Elmore copper with a confirmed purity of 99.997%. The residual resistance ratio was 1,700.

The aluminum was obtained from Vereinigten Aluminiumwerken A. G. with a purity of 99.998%.

All three metals were melted into ingots in the electron beam oven. The samples were prepared from these ingots. The pin sample had a diameter of 5 mm and a height of 19 mm. The front surface was slightly convex with a radius of curvature of r ≈ 10 mm. The rectangular comparison sample had the dimensions 43 x 13 x 5 mm. /34

Because of their high purity, and as a result of the fusion in the electron beam oven, all the samples had relatively coarse grains.

The materials were particularly selected for their capability of emitting exoelectrons. Also, the mutual frictional values for the metals are well-known, so that comparison with other authors is possible.

Iron shows practically no exoelectron emission.

Copper has a high thermoemission, but no photoemission. Aluminum has a very high photoemission, but only very weak thermoemission.

In friction experiments with these metals, the exoelectron effects to be expected can be separated well from each other.

3.7 Performance of the Measurements

All the samples were polished with diamond paste immediately before the experiment. The polishing time and diamond particle size were held constant.

In the first part of the work, the study of surface coating, the sample was heated in vacuum (better than 5×10^{-6} torr) up to 400° C. This heating of the sample before the measurement proper was necessary in order to free the sample surface of contaminants. The contaminants, which vaporize off at elevated temperature in vacuum, naturally also strike the SEM and simulate a high count rate, which under some circumstances can obscure the measured effect.

During the heating out, a thin glass plate lay between the sample and the comparison sample to prevent welding. The glass plate fell to the side as soon as the pin was moved, and did not affect the measurements. /35

The experiment proper was begun after the sample had cooled again to room temperature. Air was allowed to enter the system until the desired pressure was reached. Then the rubbing system was turned on and the coefficient of friction recorded. After the rubbing process was ended, the system was again evacuated and the measuring equipment turned on. As a rule, the measuring system, including the SEM high voltage, operated for at least 30 minutes before the glow curve was measured.

In the transfer measurements it was not necessary to heat out the samples previously, as only the photoemission of the sample was recorded. Otherwise, the course of the experiment was as described above. For transfer measurements

at a vacuum of 10^{-6} torr, the SEM was made ready to operate even before the excitation; i.e., before rubbing. Then the measurement of exoelectron emission could be started immediately after the rubbing process.

A standard 25 watt incandescent lamp served to illuminate the samples. It was 15 cm from the sample. Figure 11 shows the spectrum of the incandescent lamp.

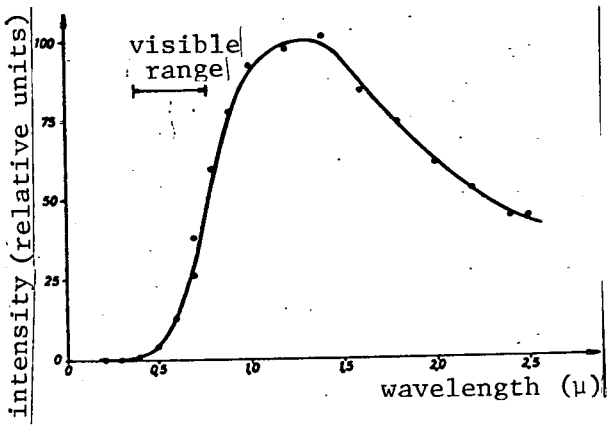

Figure 11. Glow lamp spectrum.

4. Results

4.1 Friction Measurements

In this work, the coefficient of friction was determined essentially as a function of the air pressure or oxygen pressure and of the materials used.

The measured values are summarized in Table 1, pages 38* and 39*.

The results of experiments 1 to 11 and 12 to 16 are also shown in Figure 12. Curve 2 corresponds to experiments 1 to 11. In this series of tests, the frictional coefficient for the metal pair Cu-Cu was determined. After polishing, the samples were inserted into the apparatus, and the pressure in the system was lowered to the desired value. Then the test was started without further sample treatment. Starting at normal pressure, the coefficients of friction had a relatively small value of about 0.22, which climbed slowly to 10^{-3} torr. In the pressure range beyond 10^{-3} torr there was a discontinuous jump. Several measurements were performed at some pressures. Thus, in /37
Figure 12, several results are also plotted for these values. The means are given in Table 1.

*Translator's Note: English pages 32 and 33.

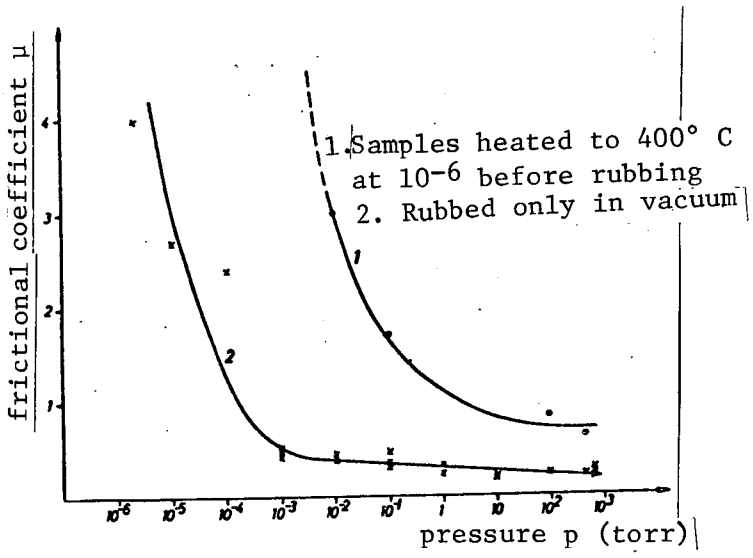

Figure 12. Frictional coefficient of copper as a function of the air pressure.

Curve 1 corresponds to experiments 12 - 16 from Table 1. These values are components of the exoelectron experiment shown in Figure 13, page 34. In these experiments the friction experiments were needed for excitation of exoelectron emission. As already described in Chapter 3.8, for these exeriments the freshly polished sample was heated to 400° C in the apparatus at a pressure below 5 x 10^{-6} torr. The experiment was performed after the cooling to room temperature.

The frictional coefficients of the samples heat-treated in this way are higher than the comparable values of curve 2. It appears that adhesive contacts occur even at the higher oxygen pressures. At 10^{-3} torr it was necessary to terminate the experiments, as the pin and sample fused together. They could not be separated again without damaging the measuring system. The measuring limits were about $\mu = 5$.

In one of the first tests in this experimental series, the sample and comparison sample were in direct contact during heating to 450° C at a pressure of 1.5 x 10^{-6} torr. After cooling, a friction experiment was to be performed at 10^{-6} torr. But the sample and comparison sample were so strongly welded that the sample mount turned instead. A force of 1.59 kp was needed to bend the mount back. With a normal load of 50 p, the "frictional coefficient" calculated from this is greater than 32.

In some of the experiments 1 - 11, microhardness was measured in parallel with determination of the frictional coefficients, and the contact area was

TABLE 1

/38

Serial No.	Pin	Sample	Pressure (torr)	Load (p)	Slide length	Heat treatment	
1	Cu	Cu	760	20,2	100	no	0,21
2	Cu	Cu	500	20,2	100	no	0,21
3	Cu	Cu	100	20,2	100	no	0,22
4	Cu	Cu	10	20,2	100	no	0,21
5	Cu	Cu	1	20,2	100	no	0,22
6	Cu	Cu	10^{-1}	20,2	100	no	0,34
7	Cu	Cu	10^{-2}	20,2	100	no	0,4
8	Cu	Cu	10^{-3}	20,2	100	no	0,46
9	Cu	Cu	10^{-4}	20,2	100	no	2,4
10	Cu	Cu	10^{-5}	20,2	100	no	2,7
11	Cu	Cu	10^{-6}	20,2	100	no	4,0
12	Cu	Cu	760	49,7	100	yes	0,61
13	Cu	Cu	100	49,7	100	yes	0,85
14	Cu	Cu	1	49,7	100	yes	-
15	Cu	Cu	10^{-1}	49,7	100	yes	1,7
16	Cu	Cu	10^{-2}	49,7	100	yes	3,0
17	Cu	Cu_2O	760	20,2	100	yes	0,31
18	Cu	CuO	760	20,2	100	yes	0,30
19	Cu	CuO	760	20,2	100	yes	0,54
20	Al	Al	760	47,8	100	yes	1,15
21	Al	Al	760	18,3	100	yes	1,18
22	Al	Al	760	18,3	100	yes	1,09
23	Al	Al	760	18,3	100	yes	1,14
24	Al	Fe	760	47,8	100	no	0,58
25	Al	Fe	2×10^{-6}	47,8	10	no	0,65
26	Al	Fe	1×10^{-6}	47,8	50	no	0,71
27	Al	Fe	1×10^{-6}	47,8	100	no	0,98
28	Al	Cu	1×10^{-6}	47,8	100	no	1,43

TABLE 1 (continued)

Serial No.	Feller [84]	Afanas'ev [85]	Braun [86]	Hinsley [15]	Rabinowicz [7]	Bowden, Tabor [5]	Habig [87]	Sikorski [1]	Tung Liu [88]
1					0,8-1,2		0,8-1,0	4,3	0,4-1
2									
3									
4									
5							1,21-1,28		
6									
7									
8							1,29-1,49		
9							1,29-1,73		
10	1,36						1,58-1,75		
11		1,56							
12			3,2			1,2			
13			3,7						
14			4,0						
15			4,2						
16			4,3						
17									
18									
19				0,57					
20		1,43						2,8	
21									
22									
23									
24							0,75-0,81		
25									
26									
27	0,98						0,78-0,88		
28	0,98								

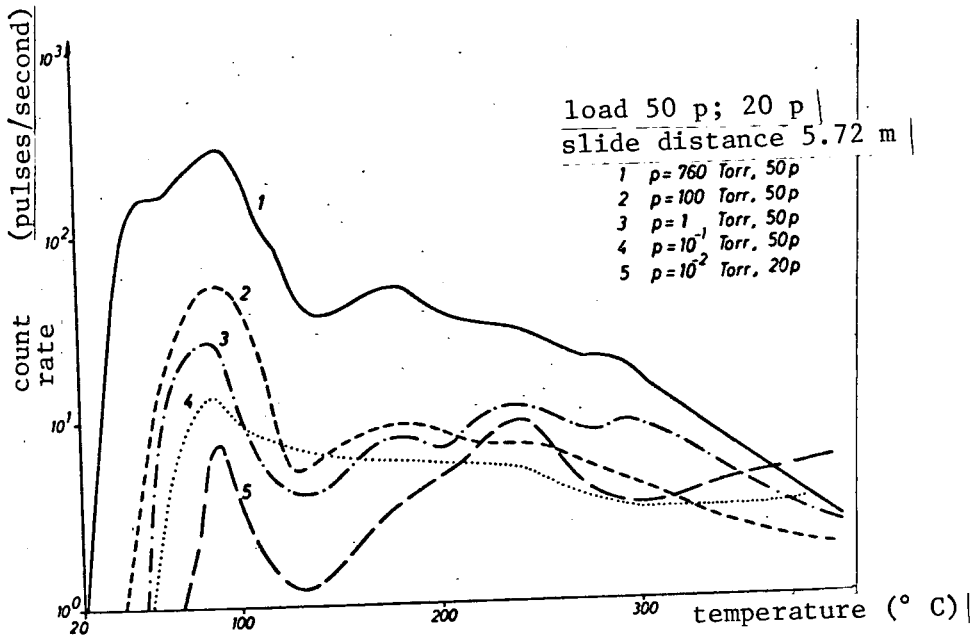

Figure 13. Glow curves of copper as a function of oxygen pressure.

determined. The contact area is designated as that area which can be recognized as a deformed zone on the polished sample after the experiment. In the experiments plotted in the lower part of curve 2 it was small ($F \sim 0.5$ mm^2). It increased strongly in the upper part of the curve at low pressure to $F \sim 5$ mm^2.

From these values and the standard load of 20.2 p, one can calculate a surface pressure of 40.4 p/mm^2 or 4 p/mm^2 for the lower or upper part of the curve. /40

The microhardness measurement yielded a hardness of 56.2 HV on the undeformed material and a hardness of 79.3 HV in the friction track after the experiment. The hardness measurement was performed with a standard load of 100 p.

Experiments 17 - 19 of Table 1 are part of the exoelectron experiments shown in Figures 14 and 15, page 43*. In these, oxidized copper samples were studied. Of experiment 19, it should be noted that the pin penetrated the oxide layer during the experiment and rubbed partially on the copper sample. In experiments 17 and 18 the oxide layer was not penetrated. The copper pin rubbed on the oxide layer.

The other values of Table 1 were determined in the study of exoelectron emission on rubbing of Al on Al (20 - 23) or in the transfer measurements for Al on Fe (24 - 28). They will not be discussed further here, as they contain no new results. To the extent that they can be compared, they agree well with other values in the literature.

Except for experiments 1 - 11, all the friction experiments were performed in dry air. The air was admitted to the apparatus through the zeolite adsorption trap. Also, the SEM cooling mantle in the system was cooled to liquid nitrogen temperature. The moisture of the air which was not caught in the adsorption trap was then frozen out with the low-temperature cooling mantle of the SEM.

Some friction values from the literature are summarized in the right portion of Table 1. As well as possible, the values were arranged according to the parameters of pressure and heat treatment in the table. Because of the different initial parameters, however, the results are not directly but only qualitatively comparable.

4.2 Exoelectron Emission

/41

Another goal of this work (see Chapter 2.3) was to investigate whether one can, by means of exoelectron emission, determine the degree and type of covering of a surface. The answer appears from the following experiments which were performed with copper. Copper is especially suited for this experiment,

*Translator's Note: English page 37.

as it shows strong thermoemission. The experiments were performed as described in Chapter 3.8. The emission rate was measured as a function of the temperature. The oxygen pressure was a parameter in the measurements.

The friction processes for excitation of exoelectron emission were performed under the same conditions in all the experiments. Figure 13 shows the result of the studies. The curves agree in showing a distinct maximum at the beginning, at about 90° C, independent of the oxygen pressure. At higher /42
temperatures more maxima appear in the curves. They agree approximately for all curves at the same temperatures. For curve 1, in this case with excitation at normal pressure, it is striking that along with the maximum at 90° C there is a smaller maximum at 60° C. None of the other curves show this first maximum.

In this work, only the first two maxima of the curves at 60° C and 90° C will be discussed. Both maxima could be assigned to unambiguously determined surface conditions, as experiments with oxidized copper samples have shown. The samples were heated in vacuum at 10^{-6} torr to 400° C. Then, with the temperature remaining the same, the pressure was increased for 10 minutes to 100 torr. Finally, the samples were cooled in vacuum at 10^{-6} torr to room temperature. The oxide layer on the surface was studied by reflection electron diffraction. It consisted only of Cu_2O. Figure 14 shows the glow curve recorded from it. The diffraction picture of the sample surface is also shown. In this experiment, the excitation for the emission of exoelectrons comes from electron impace in recording the diffraction pattern. The count rate is higher by two orders of magnitude than with excitation by friction. This effect had often been observed previously [43]. With this type of excitation, we observe the appearance of more or new maxima. The maximum in the count rate at 90° C, such as was also found in samples excited by friction, is again noteworthy.

In a further test, the copper samples were heated at 460° C for six minutes in air and finally cooled rapidly. As before, the surface of this sample was analyzed by electron diffraction, and a glow curve was recorded. The glow curve and diffraction pattern are shown in Figure 15.

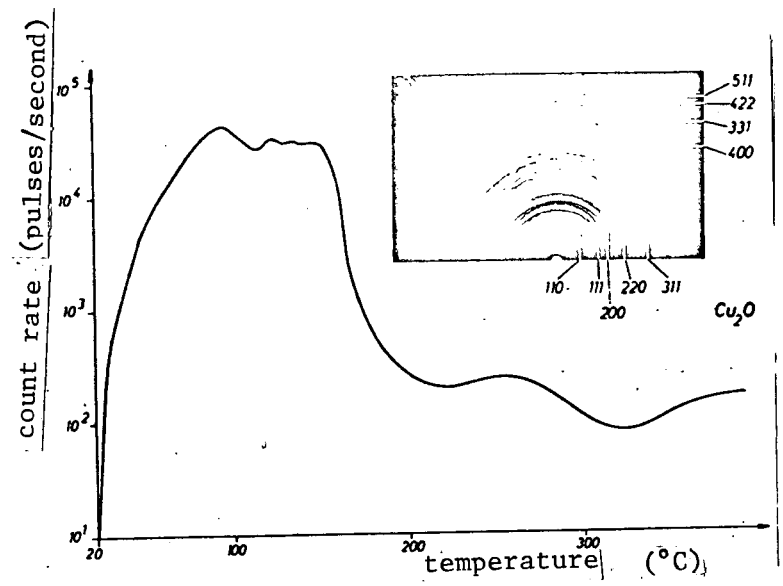

Figure 14. Glow curve of oxidized Cu (Cu_2O) with the diffraction pattern of the sample surface.

NOT REPRODUCIBLE

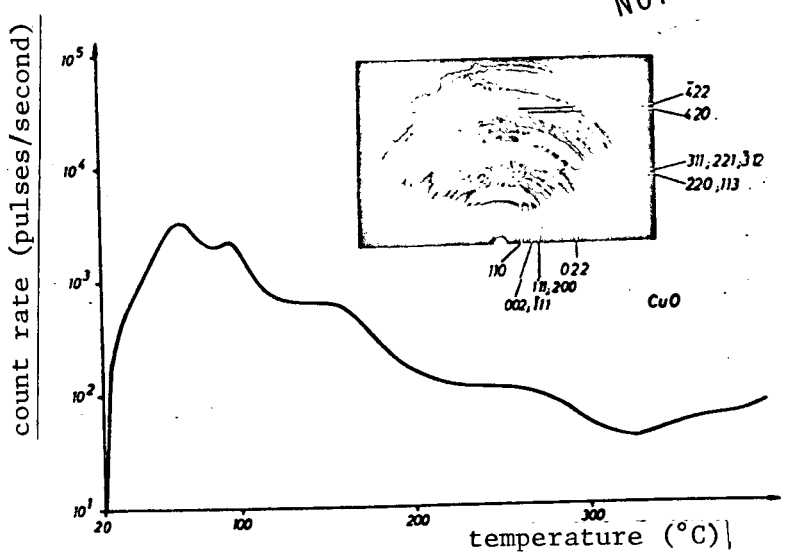

Figure 15. Glow curve of oxidized Cu (CuO) with the diffraction pattern of the sample surface.

If we compare the glow curves of copper samples with Cu_2O or CuO on the surface (Figures 14, 15), we find, aside from the height of the count rate, indications of maxima or plateaus which occur at the same temperatures for both curves above 100° C. In both curves the maxima at 90° C is present, but in the sample covered with CuO it is surpassed and partially obscured. /44

From these experiments it appears that in the presence of Cu_2O on the sample surface, the glow curve for exoelectron emission exhibits a strong maximum at 90° C, while CuO on the surface leads to a maximum in the glow curve at 60° C.

At high temperatures in oxygen-rich atmospheres, Cu_2O also forms simultaneously with CuO (see the second maximum in Figure 15 at 90° C). Conversely, only Cu_2O forms in oxygen-poor atmosphere, as Figure 15 shows.

These results agree well with the glow curves measured on polished copper surfaces after friction (see Figure 13, page 41*). With friction in air at room temperature, both oxides (Cu_2O and CuO) appear, although preferentially Cu_2O. If the samples are excited by friction at lower pressures and room temperature, then the maximum from the oxygen-rich oxide vanishes. Then only the maximum from the oxygen-poor oxide, Cu_2O, remains.

Along with the position of the maxima, their height as a function of the pressure is an important result of the experiments. For the maxima at 90° C we can read from Figure 13 a clear dependence of the count rate on the pressure. The height of the maxima decreases with decreasing pressure, as shown in Figure 16. There, the height of the maxima is shown as a function of the pressure at which the samples were excited. This gives a straight line on a log-log plot. It appears to indicate that the count rate decreases in proportion to a power of the pressure.

This statement must, however, be made with the limitation that there are only five points for the plot. In order to confirm this regularity, extensive experimental work is still necessary. /45

*Translator's Note: English page 34.

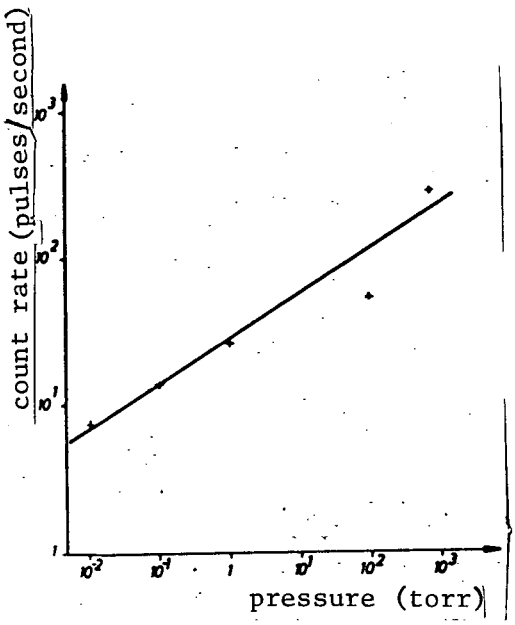

Figure 16. Height of the glow maximum at 90° C as a function of the pressure at excitation.

The samples were rubbed at the pressures given in Figure 13, page 41. The pure processing time amounted to 9 minutes and 50 seconds. After that, there were a few minutes which were needed for preparation. In all, the samples previously heated at 10^{-6} torr were exposed to the increased air pressure for 10 - 12 minutes. Finally, the glow curve was measured at 10^{-6} torr. The excitation — or, expressed more accurately, the mechanical work provided by rubbing — is thus the same in all the experiments. Only the simultaneous or subsequent process of adsorption and oxidation was different. As already has been shown, different oxides form as a result of the rubbing process at high or low partial pressures of oxygen. At the same time, the formation of the oxide layer produced at low oxygen pressures is also affected. At constant excitation conditions, the formation or thickness of the oxide layer is a function of the oxygen availability. Its growth was interrupted at the end of the processing period at a /46 layer thickness which was definite, but different for each pressure range. The slight growth at 10^{-6} torr during recording of the glow curves does not affect the test condition established during the higher pressure, as can be seen by extrapolating the line to 10^{-6} torr.

To summarize, we may say of these measurements that the count rate for exoelectron emission in the Cu_2O glow maximum is a measure of the layer thickness or the stage of growth of the oxide layer. From the previously measured values, one can conclude that there is an exponential dependence of count rate on the pressure during working.

Along with the Cu-Cu metal pair, the metal pairs Fe-Fe and Al-Al were also studied.

With iron, no emission was found with excitation by friction and electron impace (40 kV, 5 minutes). Stimulation by light, like that by heat, was unsuccessful. Emission could be measured only by tensile breaking of an iron ribbon. This effect was reproducible and is shown in Figure 17.

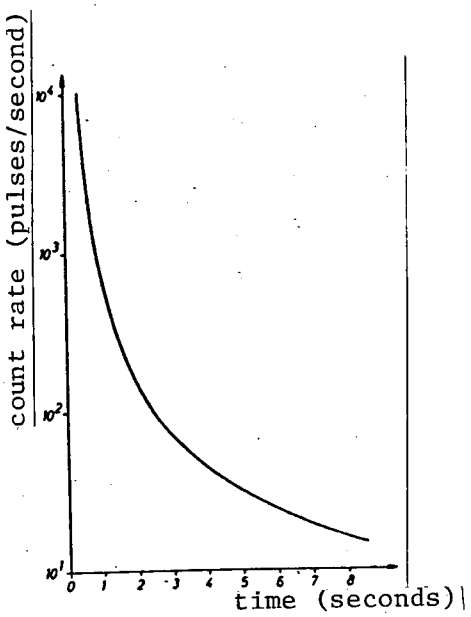

Figure 17. Decay curve of exoelectron emission after tearing apart an iron ribbon.

With aluminum, the well-known photostimulated decay curves were measured [39-43]. They will not be shown here, as they are the basis of a measuring procedure treated in the next chapter and are described there. With aluminum we were unable to obtain reasonable and reproducible glow curves by excitation with friction and electron impace. /47

4.3 Transfer Measurements

In the measurements with aluminum, a strong exoelectron emission easily stimulated by photon irradiation was found. Even a slight mechanical working sufficed to excite emission.

In contrast to iron and copper, then, aluminum shows distinct photoemission which begins immediately with the action of the light. Darkening the sample stopped the emission process, and the emission rate dropped nearly to the background rate of the recording system.

These properties of aluminum made it especially suitable for transfer experiments. The object of the experiments was to demonstrate the transfer of aluminum to iron by means of exoelectron emission. In the experiments, an aluminum pin sample rubbed on a comparison sample of iron. Iron was selected as the comparison sample because it shows only extremely slight exoelectron emission. If aluminum is transferred, it can be demonstrated through alternate illumination and darkening of the sample. To test the exoelectron experiments, the samples were finally studied by a microprobe (Cambridge Microscan). Three analyses were undertaken.

a) An electron micrograph was made of one part of the sample surface.

b) From the same sample section, the emission of the $Al_{K\ \alpha 1}$ line was recorded by the scanning procedure and photographed as a survey photograph.

c) The sample was explored point by point with the electron beam, and the emission of the $Al_{K\ \alpha 1}$ x-ray line was recorded. /48

The results of the measurements are shown in the following figures (Figure 18 - 22, pages 49-53*). In a) and c) the results of the analyses described are shown. The fourth part of the figure shows the measured exoelectron emission rate.

The electron micrograph shows the slide paths which the aluminum pin left on the iron sample. Fused-on particles can clearly be recognized in the pictures. But here we might mention one disadvantage of this electron microscopic imaging: It has a very slight depth of field. Large and high particles are recorded only as black spots. Small particles as in Figure 20 a) are still sharply imaged. In Figure 18 a) a light-microscopic picture of the sample surface, rather than an electron micrograph, is shown. In the center of the picture a broad dark streak runs horizontally. That is the burned track which the electron beam has left behind on exploring the sample along its surface. The path of the electron beam is marked with the letters A - B beside the figures in the following pictures.

*Translator's Note: English pages 42-46.

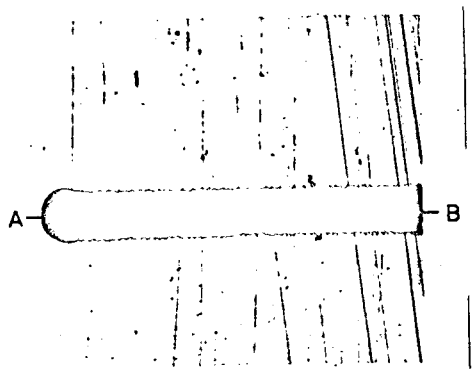

No x-ray emission detectable

a) Light-microscope picture of the sample surface

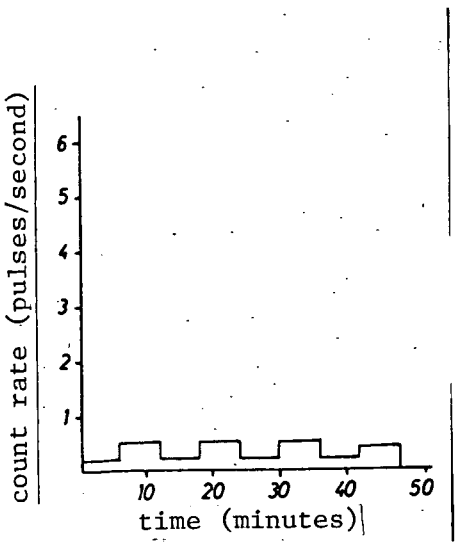

Exoelectron emission rate

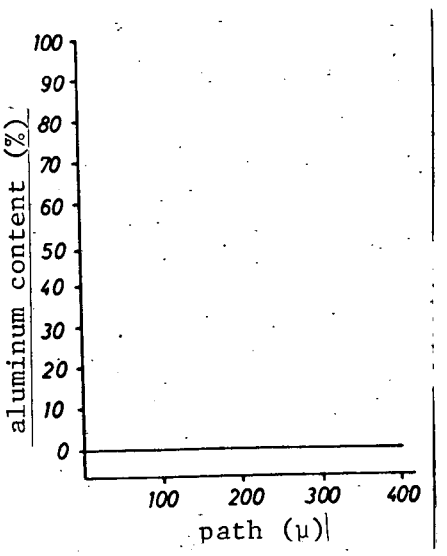

c) Aluminum transfer along A-B

Figure 18. Transfer measurement: Aluminum pin, iron sample, slide distance 100 x, 760 torr.

NOT REPRODUCIBLE

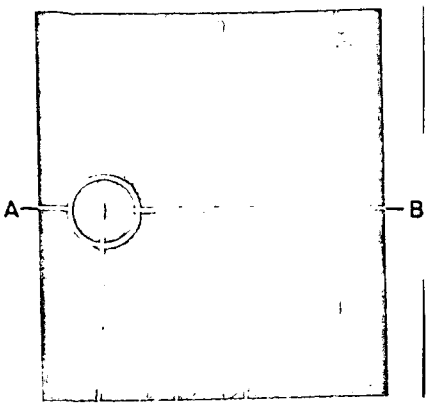

No x-ray emission detectable

a) Electron micrograph of the sample surface

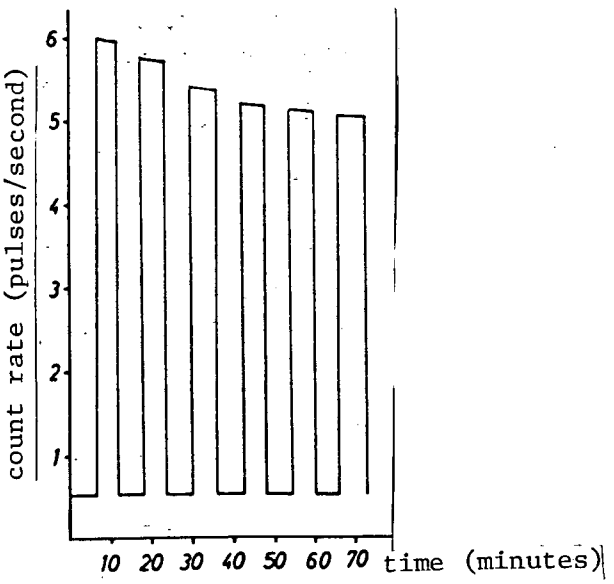

Exoelectron emission rate

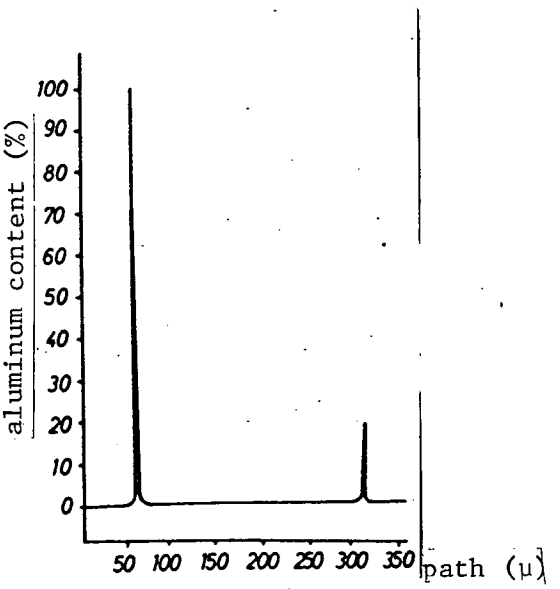

c) Aluminum transfer along A-B

Figure 19. Transfer measurement: Aluminum pin, iron sample, slide distance 10 x, 10^{-6} torr.

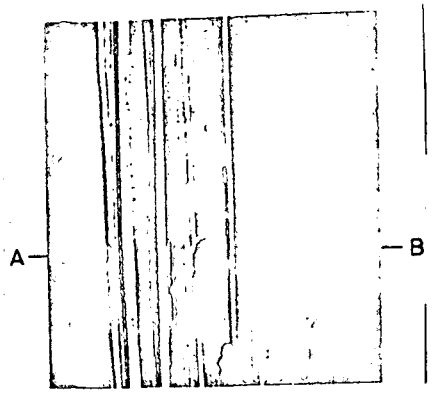

a) Electron micrograph of the sample surface

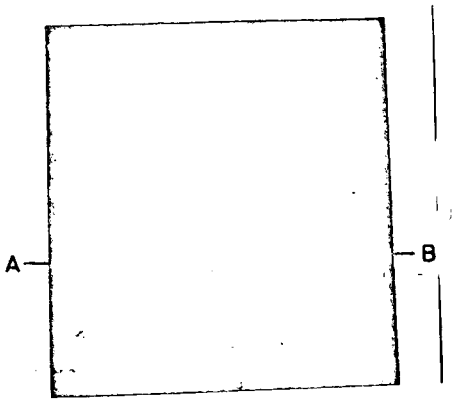

b) X-ray $Al_{K\ \alpha 1}$ emission from the sample surface

NOT REPRODUCIBLE

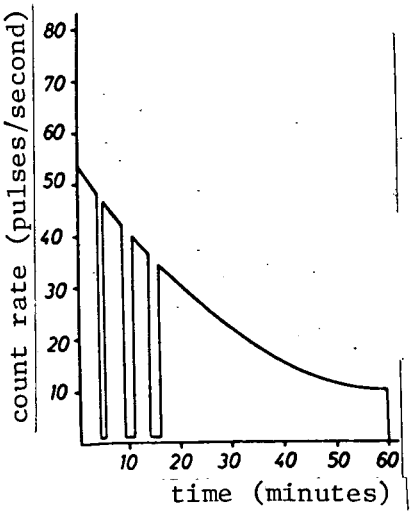

Exoelectron emission rate

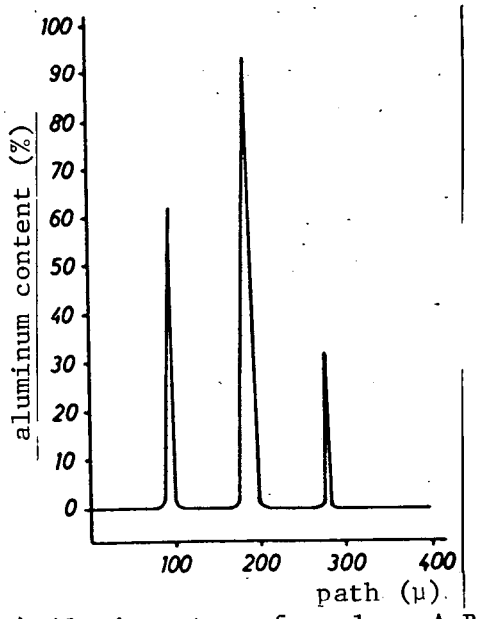

c) Aluminum transfer along A-B

Figure 20. Transfer measurement: Aluminum pin, iron sample, slide distance 50 x, 10^{-6} torr.

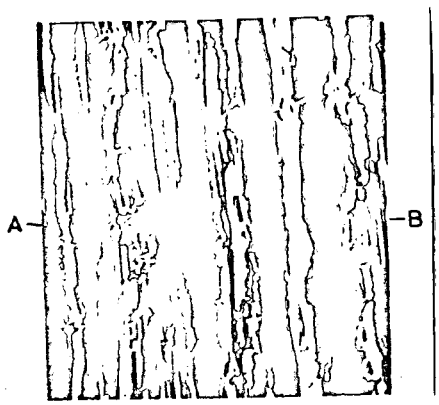

a) Electron micrograph of the sample surface

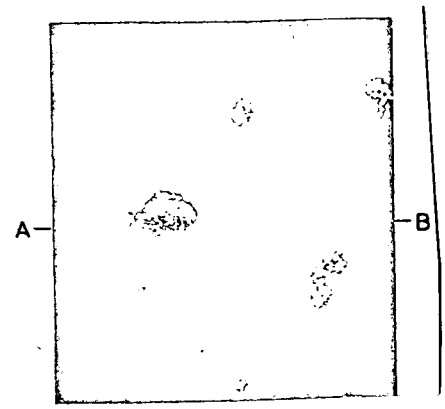

b) X-ray $Al_{K\ \alpha 1}$ emission from the sample surface

NOT REPRODUCIBLE

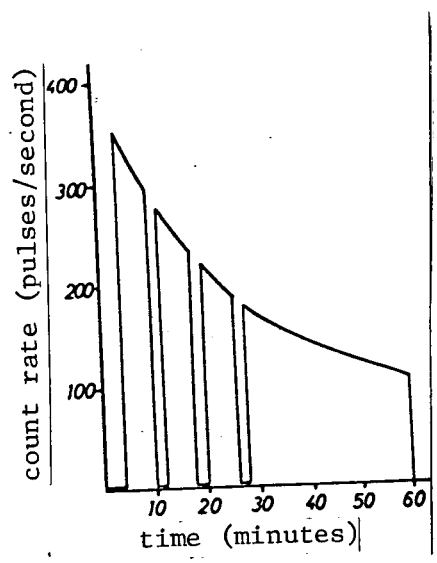

Exoelectron emission rate

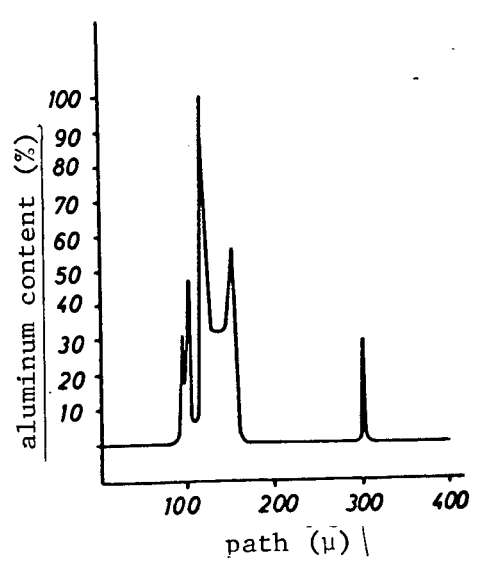

c) Aluminum transfer along A-B

Figure 21. Transfer measurement: Aluminum pin, iron sample, slide distance 100 x, 10^{-6} torr.

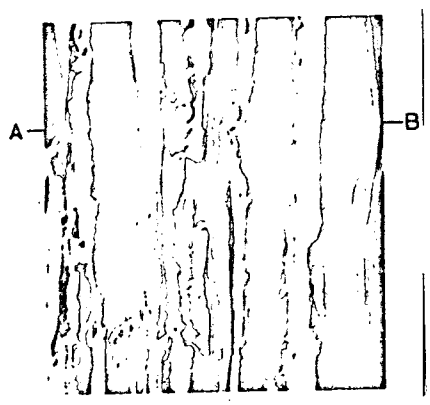

a) Electron micrograph of the sample surface

NOT REPRODUCIBLE

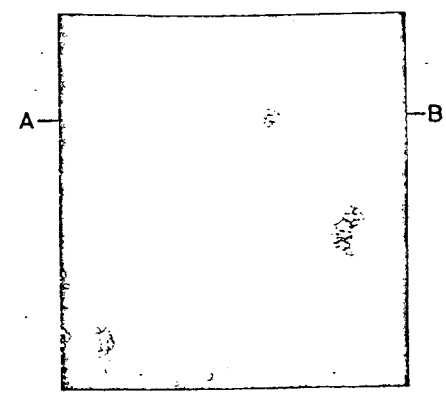

b) X-ray $Al_{K\ \alpha 1}$ emission from the sample surface

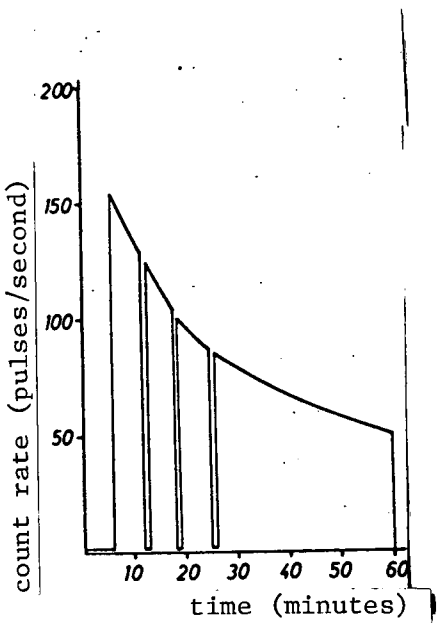

Exoelectron emission rate

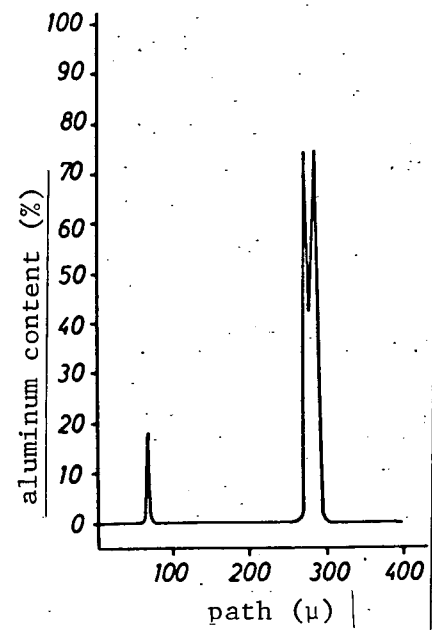

c) Aluminum transfer along A-B

Figure 22. Transfer measurement: Aluminum pin, copper sample, slide distance 100 x, 10^{-6} torr.

In the x-ray image of the sample surface, the transferred aluminum particles are bright. The x-ray image and the electron-optical image have the same coverage. By superimposition, the aluminum particles found in the x-ray image could be assigned to the electron microscopic image.

During the point-by-point exploration of the sample surface along the section A - B, the x-ray emission could be recorded. It is shown in part c) of the figures. This process is basically more accurate than the survey pictures shown in part b) of the figures. The length of the abscissa in parts c) correspond to the width of the image in parts a) and b). Thus, the maxima in the recorder diagrams c) correspond to the bright spots lying above them in the x-ray images.

Along with the microprobe pictures, the exoelectron emission rates for /54
the various experiments are shown in Figures 18 - 22. Figure 18 shows the result of a friction experiment which was performed in air. Only slight scratches can be seen in the light microscope picture. No transfer is demonstrable with the microprobe. The exoelectron emission rate shows the null effect. This is the count rate which was measured before each friction experiment. The increased regions in the count rate correspond to the time periods in which the sample was illuminated. In the lower regions, the probe was correspondingly darkened.

The first transfer is demonstrable in Figure 19. The test matching that figure, like all the following tests, was carried out in vacuum at 10^{-6} torr. The pin sample was moved 10 times across the iron sample. In this experiment it is interesting that no transfer can yet be detected in the x-ray image from the microprobe, although there is exoelectron emission. In both the following pictures (20, 21) the number of rubbing periods was increased to 50 or 100. The sliding traces and the transfer increase strongly. Likewise, the count rate for exoelectron emission increases. The notches in the curves correspond to the times during which the sample was darkened. These controls were performed in order to show that the emission came from the transferred aluminum.

In the last figure (Figure 22), results are shown from an experiment with the metal pair: Al pin, Cu sample. This was to demonstrate that the method of transfer measurement described here is not limited to the Al-Fe metal pair. Rather, it can be applied with all metal pairs in which the exoelectron emission rates of the friction partners can reliably be distinguished from each other by different stimulation (photons, heat, electron impact).

5. Discussion /55

5.1 Friction Measurements

The results of the friction measurements are summarized in Table 1, pages 38 and 39. They are in part plotted in Figure 11, page 35*.

The difference between curves 1 and 2 in Figure 11 is in the heat treatment to which the samples of curve 1 were exposed. As a result, there appears a higher coefficient of friction. Even at relatively high pressures, seizing to the friction partner occurs.

These results can be related back to two causes:

1. By heating out in the vacuum, the sample is thoroughly freed of impurities which lie on the surface. In preliminary experiments it was observed that even layers of tarnish can be removed in this way. To be sure, a new layer forms on the sample surface during cooling back to the beginning of the experiment; but it never has the same thickness as a layer formed in air in the same period. Furthermore, we can assume that surface oxide coatings produced under different experimental conditions can differ in their mechanical properties.

2. Along with destruction of the nonmetallic surface layers, heating in vacuum also produces a decrease in hardness. The samples were "annealed". This effect is very distinct with copper.

*Translator's Note: English page 30.

In a following friction experiment, the thinner nonmetallic surface layer on the sample is penetrated earlier. Metallic contact and strong adhesion occur. The coefficient of friction increases. Because of the low hardness of the tempered material, the elastic range of deformation is rapidly exceeded, and plastic deformation occurs. The result of this is an enlargement of the contact area. In all, a greater force is needed to separate the fused contact bridges.

Both effects, the thinner oxide layer and the lower hardness, lead to a higher coefficient of friction in the case of curve 1. /56

The decrease in hardness on annealing is responsible for the higher frictional value at normal pressure. The originally thinner oxide layer on the sample has only a slight effect on the frictional coefficient in a friction process under normal pressure, because the oxide layer is immediately reformed on the surface after penetration and scraping off, independent of the layer which occurred on the surface previously.

With decreasing pressure, the effect of the "clean surface" becomes increasingly stronger. It adds to the increase in frictional coefficient produced by the lower hardness. The result is a sudden increase in the coefficient of friction to very high values.

In curve 2 of Figure 11, the coefficient of friction is about $\mu = 0.22$ in the range from 760 torr to 10^{-2} torr. The time course of the tangential force on rubbing was rather constant. After the friction experiment, only a few sharply limited grooves could be seen on the sample. The region attacked on the comparison sample was small and relatively smooth. It can be assumed that the pin ran along the surface layer of the comparison sample and that this acted as a lubricating layer.

The external appearance of friction changed fundamentally in the pressure range from 10^{-3} to 10^{-4} torr. The tangential force shows sharp peaks typical of stick-slip movements. It was observed that the pin sample moved jerkily

over the comparison sample. After the frictional experiment, deep grooves and fused-on particles appear both on the sample and on the pin, similar to those shown in Figure 20 a, page 44 and Figure 21 a, page 45, for Al-Fe. From these results it must be concluded that in the pressure range from 10^{-3} to 10^{-4} torr the surface coating on the sample is penetrated and metal-metal contact occurs, leading to stronger adhesion and welding.

In the right portion of Table 1, there are summarized literature values of coefficients of friction reported by some authors. The values are in part /57
quite different, and it is difficult to compare them with each other, as the authors have proceeded from different assumptions. Feller et al. [84] and Afanas'ev and Khimich [85], Brown and Burton [86], and Habig, Kirschke, Maennig and Tischer [87] made measurements in vacuum, and heated part of the samples. Hinsley, Male and Rowe [15], as well as Rabinowicz [7] and Tung-Liu [88], performed their experiments in air, as did Sikorski [1]. Sikorski pressed the faces of rod-shaped samples together and rotated them. In this process, he immediately penetrated the surface layer of the sample and produced plastic deformation. Thus, he obtained friction and adhesion coefficients otherwise measured only in high vacuum.

The values of Habig, Kirschke, Maennig and Tischer[(1)] were measured at a standard load of 1.2 kp and after a run-in process one km in length. The surface pressure, calculated from the areas in contact, was comparable in their and our experiments. Nevertheless, the form of the abrasion phenomenon differed in the two experiments. Habig et al. found even at normal pressure that there were severe abrasion phenomena on the pin and the disk after the run-in process. In our experiments, there was hardly any attack on either the pin or the sample. Slide paths could be seen only with great difficulty by means of the naked eye.

---

(1) At this point we heartily thank those authors for kindly providing their experimental values.

In our experiments, we were apparently in the abrasion region which was earlier characterized as "mild wear", while Habig et al. made their measurements in the range of "severe wear". These differences were possible, because the true contact areas are not known for the experiments. In the region of individual contact bridges, however, it is the actual standard load which is important and not the calculated surface pressure. The normal loads applied differed in the two experiments from 1.2 kp for Habig to 20 p for our measurement.

This difference may perhaps also make the differences in the results of the other authors understandable. Without exception, they measured higher values at normal pressure for the Cu-Cu friction system. In spite of these /58
different assumptions, there is in part good agreement of our values with those of other authors.

5.2 Exoelectron Emission

5.2.1 Experimental

With the results described in Chapter 4.2, it could be demonstrated that the exoelectron emission is a function of the rate of covering of the metal surface. This experiment was performed with copper. It showed that definite maxima in the glow curves always appear at the same temperature. The number of maxima and their relative position is a recognition characteristic for each metal.

The individual maxima are characteristic of various surface conditions of the sample. The principal maxima could unambiguously be recognized as a function of the oxide coating of the sample. With coating of the surface with CuO (demonstrated electronoptically) there was a high maximum at 60° C, which was also found in friction experiments in air. In friction experiments performed at 100 torr and below, only Cu_2O can be demonstrated on the surface. The supply of air oxygen is so small that only the oxygen-poor oxide is formed.

The height of the Cu_2O maximum at 90° C can be interpreted as a measure of the thickness of the oxide layer. But it is not yet possible to derive an absolute statement of the thickness of the layer from the experiments made here alone. For that, it is yet necessary to have a series of comparative and analytic experiments. From our experiments, we can primarily conclude only that there is an exponential dependence of the count rate on the pressure during the friction process. Proceeding from this result, then, a relation to the layer thickness must be found. Recognition of this relation requires a suitable experimental investigation. But we can certainly determine it, because the physical basis of exoelectron emission lies in the formation and growth of the oxide layer. The pressure dependence itself implies the relations with formation. /59

Studies on the relation between the thickness of the oxide and the exoelectron emission for copper oxide have already been made by Müller [89]. But his results cannot be compared with these, because he used other experimental conditions, stimulation in air by x-ray irradiation, and he also registered the exoelectrons with a Geiger-Müller counter in a counting gas atmosphere.

5.2.2 Theoretical Considerations

On the basis of our results and the literature reported in Chapter 2.2, we can now describe a comprehensive concept for the theory of exoelectron emission, in which the known results can be arranged without forcing.

Ramsey [39] and recently,also, Linke and Meyer [90] have shown convincingly in their work that in the initial stages of emission, the covering of the surface with a monoatomic layer of oxygen and water is necessary for the occurrence of the emission. The adsorbed water molecules form a dipole layer which reduces the work function so that the exoelectron emission for this stage can be explained as a photoeffect with a shifted limiting wavelength.

In these experiments, the times measured for attaining the maximum emission are astonishingly large. At 10^{-7} torr the time needed was 41 minutes (Ramsey) and 16 minutes 40 seconds (Linke, Meyer). Linke and Meyer explain this long build-up time through the formation of an oxygen layer by the action of water. They base this on the works of Huber and Kirk [44] as well as Eley and Wilkinson [91]. The subsequent drop in emission is dependent on the partial pressure of oxygen. It occurs more rapidly, the higher the oxygen pressure is.

These measurement results of Ramsey and Linke and Meyer, as well as our /60
own measurements, will be the initial points of departure for the model of the exoelectron emission from metal surfaces discussed here.

After adsorption of water and the accumulation of oxygen which follows, as has been discussed by the referenced authors, a diffusion process does take place without a doubt which transports the metal atoms into the chemically absorbed layer. The beginning of this diffusion process can be imagined as a location-change reaction between the adsorbed oxygen and the metal atoms. It is assumed that when then this oxide layer begins to grow, lattice defects are produced, which have stable electron terms having a higher energy than the metal or the oxide respectively.

These lattice defects can be primarily vacancies, but other types of lattice defects are possible. Vacancies will also wander into the surface layer. However, they are of no consequence for the size of the emission, as Müller and Pontinen [38] have shown. These lattice defects constitute the source of the exoelectron emission for surfaces covered with oxides.

In order to interpret the glow curves, it is expedient to assume vacancies which become lattice disturbances of the F-center type. F-centers are anion vacancies, which are occupied by an electron. The F-centers are assumed, because the F-centers are well-known disturbances in the case of luminescence phenomena. The electrons can form an atom-like bond with the positive neighboring ions.

This configuration has stable energy terms, which are immediately below the conduction band [92]. The electrons which are captured in these F-centers are no longer freely moveable. However, they can only fall back into these valency band via the conduction band. This means that they are stored.

If these storage positions are emptied by energy supply, then the electrons will first again reach the conduction band of the oxide. Various processes can now occur: 1.) One part of the electrons can fall back into the vacancies. 2.) Electrons recombinate while emitting light with an activator term (luminescence). 3.) Electrons in the conduction band increase the conductivity. /61 4.) Electrons are emitted as exoelectrons. In our discussion, we will only consider point 4.).

In order to interpret the pulsed emission, it is assumed that vacancies wander to this surface and there become centers having a lower work function. They form surface terms, the energy levels of which lie just below the vacuum limiting energy and make possible for the electrons to escape from the metal bond, if energy is supplied, for example, by means of incoming light. The surface terms can be not only vacancies, but Ad-atoms and/or dipole regions are thinkable as well. It is only important that centers having a reduced work function are produced on the surface.

The emission process can be thought of as follows: The covering layers are scraped off the probe surface by mechanical working. A clean metal surface is produced. An energy model such as is shown in Figure 23 a) corresponds to it.

At the same time, according to Ramsey, Linke and Meyer, regions having a low work function are formed by adsorption of a monomolecular water layer on the clean surface. It should be recalled that a non-metallic covering layer is located on the probe surface at the beginning of the emission.

Because of the reduced work function and the effect of the light, electron emission from the conduction band of the metal can occur from these very thin layers. The non-metallic covering layer can be easily penetrated by the electrons at this stage. The counting rate is high (Figure 23 b).

As the surface layer thickness increases, the region having a lower function is reduced in size by absorption of oxygen. In this way, the counting rate (see Figure 3, page 14) drops. At the same time, oxide formation commences, and the possiblility that the electrons can penetrate the growing oxide layer decreases. In the case of large oxide thicknesses, they must be lifted into the conduction band of the oxide, in order to escape from there with energy supply via a surface trap (Figure 23 c). The mechanical energy for the friction deformation of the metal surface constitutes the excitation energy for the electrons.

/62

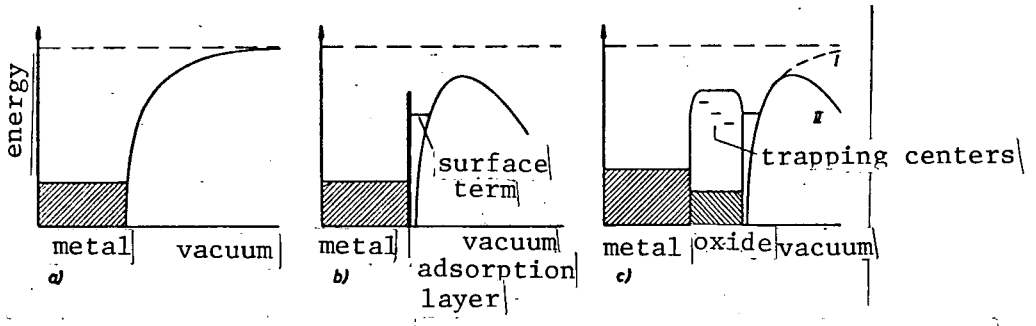

Figure 23. Schematic energy band model for exoelectron emission.

a. clean metal surface
b. metal surface with adsorbed water layer
c. oxidized metal surface

Emission from a trapping center is more probable on statistical grounds, since the trapping center is ascribed a stable high energy level. The probability for an electron stopping at a trapping center, and thus of interaction with a photon, is very high, in contrast to that of an electron in the conduction band of the oxide.

The surface energy of an oxidized metal surface is shown in curve I of Figure 23 c. In order to maintain emission, new trapping centers or sites of decreased work function must be produced continuously. The presence or formation of such sites leads to the curve for surface energy shown in curve II, /63 Figure 23 c. According to the assumption made, the emission centers are supposed to be lattice defects which migrate to the surface and heal there.

For greater layer thicknesses, emission becomes a diffusion-controlled process.

The model of exoelectron emission described above will now be applied to the experimentally observed effects.

The drop in emission with time, described by the decay curves, can be understood in the model as the phenomenon of transport of lattice defects to the oxide-gas limiting surface. With increasing thickness of oxide, this transport process is extensively limited, and the emission rate drops. The number of defect sites in the oxide layer also decreases due to migration to the surface and recombination. Emission becomes exhausted if the defect excess in the oxide layer is healed and no electrons are furnished from the crystal combination.

The possibility of storage of the exoelectrons and thus the occurrence of glow curves was already described. Electrons which arrive at the conduction band of the oxide can be stored in trapping sites in the oxide layer. On heating of the sample, they can return to the conduction band and be emitted as exoelectrons. The increase of the glow maxima with increasing pressure during working is easily explained from the thicker oxide layer formed during the friction process. This increases the absolute number of defects which can act as potential electron trapping centers.

The model developed here can also be applied to the different emission characteristics of individual metals. In the experiment it was observed that,

for instance, copper shows a distinct thermoemission, but no emission during or after working. For aluminum, the emission characteristics are exactly reversed. These different emission behaviors can be explained if one assumes that the metal oxides form trapping centers and surface terms of different depths. For aluminum it is assumed that most of the trapping centers are so close below the conduction band that they are vacated even at room temperature. Electron storage can hardly occur. The excited electrons are emitted immediately. For copper, analogously, it is assumed that there are in the oxide a large number of trapping centers lying low enough so that the electrons arriving in the oxide conduction band are essentially stored. /64

The assumption of very shallow trapping centers in aluminum was confirmed by Claytor and Brotzen [93]. These authors stimulated aluminum by mechanical working at liquid nitrogen temperature, and then warmed it. They found an emission maximum at -70° C.

The prediction that emission is minimal during and after deformation of copper because the position of the trapping centers in the oxide between the valence and conduction bands is low, can be confirmed by an experiment at elevated temperature. Stronger post-emission must then be demonstrable.

5.3 Transfer Measurements

Exoelectron emission has been shown to be an effective study method for determining the transfer from one friction partner to the other. The sensitivity is comparable with that of the microprobe for point by point exploration of the sample.

In the experiments performed here, we could not record exoelectrons with maximum sensitivity because of the apparatus. The amplification of the secondary electron multiplier was below its maximum value, and long-wave light was used for illuminating the sample (see Figure 10). For optimal matching of the light source and recording equipment, a further increase in sensitivity is to be expected.

Even with its limitations, determination of transfer by measurement of exoelectrons is comparable with the method of radioactive labeling, without the necessity of the precautionary measures which must be applied in that method. /65

6. Summary /66

With this work it can be shown that the exoelectron emission can be applied with good success to the investigation of metal surfaces in friction and abrasion processes.

For the systems Cu-Cu, Cu-Cu_2O, and Cu-CuO, electron emission was studied after stimulation by a friction experiment, and the surface coating was analyzed by reflection electron diffraction. For the system Cu-Cu, the glow curve of exoelectron emission was also measured as a function of oxygen pressure during working.

The results of the experiments in the systems Cu-Cu_2O and Cu-CuO show that exoelectron emission is a sensitive instrument for determining the type of oxide coating. The different oxides on the sample surface correspond to different maxima in the glow curve for exoelectron emission, which occur at different but characteristic temperatures.

These results were confirmed by study of the Cu-Cu system at different oxygen pressures. Both oxides, Cu_2O and CuO, appear on friction in air. When the pressure is lower, only Cu_2O appears.

The height of the maximum representative of Cu_2O decreases with decreasing oxygen pressure during mechanical frictional deformation. The experiments indicate that the count rate is a power function of the pressure. Should this relation be confirmed, exoelectron emission can be developed into a measuring method for determining the thickness of oxide layers.

Exoelectron emission can find immediate practical application in transfer measurements. The systems Al-Fe and Al-Cu were studied. The aluminum transferred to the comparison sample during the friction process can be detected in /67
the slightest amounts. The sensitivity matches that of a microprobe. Transfer can be determined during the experiment.

Although quantitative description of exoelectron emission is not yet possible, the application of this effects in the study of metal surfaces leads to new knowledge and deeper understanding of processes at the phase boundaries of solid with gas (adsorption, chemisorption, oxidation) and solid with solid (adhesion, friction, abrasion).

7. REFERENCES

1. Sikorski, M.E. Mechanism of Solid Friction. P.J. Bryant, M. Lavik, G. Salomon, Editors. Elsevier Publishers Company, 1964.

2. Documentation for Wear, Friction, Lubrication. Federal Agency for Material Testing, Berlin, Vol. 1, 1967, Vol. 6, 1969.

3. Buckley, D.H. ASLE Transactions, Vol. 11, 1968, p. 89.

4. Keller, D.C., Jr. J. of Adhesion, Vol. 1969, p. 143; Vol 1, 1969, p. 164.

5. Bowden, F.P. and D. Tabor. The Friction and Lubrication of Solids. Claredon Press, Oxford, 1964.

6. Tabor, D. Friction and Wear. Collection: Proc. Internat. Symposium on Lubrication and Wear, Houston, 1963, Herausgeber D. Muster, B. Sternlicht. Berkeley: Mc.Cutchan Publ. Corp., 1965, p. 103.

7. Rabinowicz, E. ASLE Transactions, Vol. 10, 1967, p. 400.

8. Peterson, M.B., J.J. Florek and R.E. Lee. ASLE Transaction, Vol. 3, 1960, p. 101.

9. Foley, R.T., M.B. Peterson and C. Zapf. ASLE Transactions, Vol. 6, 1963, p. 29.

10. Buckley, D.H. and R.L. Johnson. NASA Techn. Note D 1103, 1961.

11. Kingsbury, E.P. and E. Rabinowicz. Trans. ASME D 81, 1959, p. 118.

12. Klemgard, E.N. Lubrication Eng., Vol. 16, 1960, p. 468.

13. Johnson, R.L., D. Godfrey and E.E. Bisson. NASA TN 1442, 1947.

14. De Gee, A.W.J. Materialprüfung, Vol. 9, 1967, p. 166.

15. Hinsley, C.F., A.T. Male and G.W. Rowe. Wear, Vol. 11, 1968, p. 233.

16. Fehling, J.R. and N.K. Sarkar. Wear, Vol. 14, 1969, p. 33.

17. Bellinger, A. and A.W.J. de Gee. ASLE Trans., Vol. 10, 1967, p. 124.

18. Coffin, L.F. Lubrication Eng., Vol. 12, 1956, p. 50.

19. Habig, H. Federal Agency for Material Testing Berlin, Friction Section, 1968.

20. Buckley, D.H. and R.L. Johnson. ASLE Transactions, Vol. 9, 1966, p. 121.

21. Buckley, D.H. ASLE Transactions, Vol. 10, 1967, p. 134.

22. Buckley, D.H. J. Appl. Phys., Vol. 39, 1968, p. 4224.

23. Buckley, D.H. Z. Kobalt, Vol. 38, 1968, p. 17.

24. Buckley, D.H. NASA TMX-52623, 1969.

25. Buckley, D.H. J. Adhesion, Vol. 1, 1969, p. 264.

26. Buckley, D.H. NASA TN D-4775, 1968,

27. Görlich, P. and M. Ludwig. Phys. stat. sol., Vol. 28, K 117, 1968.

28. Kramer, J. Z. für Physik, Vol. 125, 1949, p. 739. /69

29. Kramer, J. Z. für Physik, Vol. 128, 1950, p. 538.

30. Kramer, J. Z. für Physik, Vol. 129, 1951, p. 34.

31. Kramer, J. Der metallische Zustand (The Metallic State). Vandenhoeck und Ruprecht, Göttingen 1950.

32. Haxel, O., F.G. Houtermans and K. Seeger. Z. für Physik, Vol. 130, 1951, p. 109.

33. Grunberg, L. and K.H.R. Wright. Acta Phys. Austriaca, Vol. 10, 1957, p. 375.

34. von Voss, W.D. and F.R. Brotzen. J. Appl. Phys., Vol. 30, 1959, p. 1639.

35. Claytor, R.N., J.E. Gragg and F.R. Brotzen. J. Appl. Phys., Vol. 37, 1965, p. 149.

36. Ku, T.C. and W.T. Pimbley. J. Appl. Phys., Vol. 32, 1961, p. 124.

37. Pimbley, W.T. and E.E. Francis. J. Appl. Phys., Vol. 32, 1961, p. 1729.

38. Müller, R.K. and K. Pontinen. J. Appl. Phys., Vol. 35, 1964, p. 1500.

39. Ramsey, J.A. Surface Science, Vol. 8, 1967, p. 313.

40. Ramsey, J.A. and G.F.J. Garlick. Brit. J. Appl. Phys., Vol. 15, 1964, p. 1353.

41. Ramsey, J.A. The Journal of the Australian Institute of Metals, Vol. 10, 1965, p. 23.

42. Ramsey, J.A. J. Appl. Phys., Vol. 37, 1966, p. 452.

43. Scharmann, A. and G. Seibert. Z. für Physik, Vol. 183, 1965, p. 249.

44. Huber, E.E. and C.T. Kirk. Surface Science, Vol. 5, 1966, p. 447.

45. Nassenstein, H. and R. Menold. Acta Phys. Austriaca, Vol. 10, 1957, p. 453.

46. Nassenstein, H. Z. Naturforschung, Vol. 10a, 1955, p. 944.

47. Baazov, D.I., Yu.A. Kolbanovskii and L.S. Polak. Kinetiki i Kataliz, Vol. 10, No. 2, 1969, p. 228.

48. Baazov, D.I., Yu.A. Kolbanovskii and L.S. Polak. Kinetika i Kataliz, Vol. 9, No. 4, 1968, p. 949.

49. Minchev, K.I. and I.V. Krylova. Kinetika i Kataliz, Vol. 9, No. 3, 1968, p. 643.

50. Ustinova, T.S. and I.V. Krylova. Russian Journal of Physical Chemistry, Vol. 42, 1968, p. 1101.

51. Ustinova, T.S. and I.V. Krylova. Russian Journal of Physical Chemistry, Vol. 42, 1968, p. 1111.

52. Senoo, S, N. Sato and T. Okamoto. Shokubai (Catalyst), Vol. 8, 1966, p. 253.

53. Sato, M. and N. Seo. Nature, Vol. 216, 1967, p. 361.

54. Kortov, V.S. and R.I. Mint. Fiz. Metal metalloved, Vol. 19, 1965, p. 877. /70

55. Kortov, V.S., R.I. Mint and I.N. Bogachev. Metallovedeniye i Termicheskaya Obrabotka Metallov, Vol. 7, 1966, p. 68.

56. Kortov, V.S. and R.I. Mint. Zavodskaya Laboratoriya, Vol. 32, 1966, p. 1144.

57. Kortov, V.S. and R.I. Mint. Izvestiya Akad. Nauk SSSR Metally, Vol. 8, 1967, p. 2.

58. Kortov, V.S. and R.I. Mint. Khimiya Metallurgiya, Vol. 12, 1967, p. 90.

59. Bogachev, I.N., V.F. Yegolayev, V.S. Kortov and R.I. Mint. Fiz. metal. metalloved, Vol. 23, 1967, p. 674.

60. Kortov, V.S. and R.I. Mint. Fizika Tverdogo Tela, Vol. 9, 1967, p. 1828.

61. Kortov, V.S. and R.I. Mint. Metallovedeniye i Termicheskaya Obrabotka Metallov, Vol. 9, 1968, p. 10.

62. Sujak, B. and J. Mader. Acta Physica Polonica, Vol. 19, 1960, p. 179.

63. Sujak, B. Acta Physica Polonica, Vol. 20, 1961, p. 889.

64. Gieroszynski, A. and B. Sujak. Acta Physica Polonica, Vol. 28, 1965, p. 311.

65. Sujak, B., A. Gieroszynski and R. Gajada. Acta Physica Polonica, Vol. 28, 1965, p. 329.

66 Gieroszynski, A. and B. Sujak. Acta Physica Polonica, Vol. 28, 1965, p. 337.

67. Gieroszynski, A. and B. Sujak. Acta Physica Polonica, Vol. 28, 1965, p. 311.

68. Lewowska, L. and B. Sujak. Acta Physica Polonica, Vol. 28, 1965, p. 483.

69. Gieroszynski, A. and B. Sujak. Part I: Acta Physica Polonica, Vol. 29, 1966, p. 275. Part. II: Acta Physica Polonica, Vol. 29, 1966, p. 523. Part. III: Acta Physica Polonica, Vol. 29, 1966, p. 533.

70. Sujak, B., T. Gorecki, M. Mathiewicz and I. Stepnoiwski. Acta Physica Polonica, Vol. 20, 1966, p. 51.

71. Biernacki, L., T. Gorecki and B. Sujak. Acta Physica Polonica, Vol. 32, 1967, p. 193.

72. Gieroszynski, A. and B. Sujak. Acta Physica Polonica, Vol. 35, 1969, p. 667.

73. Biernacki, L. and B. Sujak. Acta Physica Polonica, Vol. 35, 1969, p. 679.

74. Hempel, M., A. Kochendörfer and A. Tietze. Archiv für das Eisenhüttenwesen, Vol. 35, 1964, p. 465.

75. Koch, P. Research Reports of the Commercial and Traffic Ministry Nordrhein-Westphalia, No. 96, 1954.

76. Kramer, J. Z. für angew. Physik, Vol. 22, 1967, p. 272. /71

77. Scharmann, A. W. Kriegseis. Phys. stat. sol., Vol. 33, K41, 1969.

78. Bauer, E. Elektronenbeugung (Electron Diffraction). Verlag moderne Industrie, München, 1958.

79. Räther, H. Elektronenbeugung (Electron Diffraction). Hendbuch der Physik Band, Vol. 32, Springer Verlag, 1957.

80. Boersch, H. Z. für Physik, Vol. 130, 1951, p. 517.

81. Ruska, E. and M. Knoll. Z. für techn. Physik, Vol. 12, 1931, p. 389, 448.

82. Ruska, E. Z. für Physik, Vol. 89, 1934, p. 90.

83. Picht, J. and J. Heydenreich. Einführung in die Elektronenmikroskopie (Introduction to Electron Microscopy). VEB-Verlag Technik, Berlin, 1966.

84. Dübler, H., H.G. Feller, K. Hack and E. Matschat. To be published shortly in Z. f. Metallkunde

85. Afanas'ev, V.F. and G.S. Khimich. Fiziko-Khimicheskaya Mekhanika Materialov, Vol. 2, 1966, p. 209.

86. Brown, R.D. and R.A. Burton. Transactions of the ASME, Vol. 21, 1966, p. 1.

87. Habig, K.H., K. Kirschke, W. Maennig and H. Tischer. Federal Agency for Material Testing, Berlin, Private Communication.

88. Tung Liu. Mechanisms of Solid Friction. P.J. Bryant, M. Lavik, G. Salomon, Editors. Elsevier Publishers Compagny, 1964.

89. Muller, H. Acta Phys. Austriaca, Vol. 10, 1957, p. 474.

90. Linke, E. and K. Meyer. Surface Science, Vol. 20, 1970, p. 304.

91. Eley, D.D. and P.R. Wilkinson. Proc. Roy. Soc., London, Vol. A 254, 1960, p. 327.

92. Pohl, R.W. Introduction to Physics. Volume three. Springer Verlag Berlin, Göttingen, Heidelberg.

93. Claytor, R.N. and F.R. Brotzen. J. Appl. Phys., Vol. 36, 1965, p. 3549.

This work was done in the Institute for Metal Physics of the Technical University.

I thank Institute Director, Prof. Dr. rer. nat. H. Wever for the opportunity provided me to do this work in the Institute, as well as for his kind support.

Prof. Dr. rer. nat. H. G. Feller deserves my special thanks for setting the theme of this work, for his generous support during the performance of it, and for the stimulation and counsel of his lectures.

I thank Prof. Dr. phil. H. Boersch for providing me with the plans for the cathode he developed.

The microprobe studies were done in the Electron Microscope Laboratory of the Faculty for Mining and Refining. I thank the Director, Prof. Dr. rer. nat. M. Feller-Kniepmeier.

I also thank Mrs. E. Matschat, and all the other members of the Institute who have contributed to the performance of this work.

I thank the German Research Society for support with personnel and equipment.

Translated for National Aeronautics and Space Administration under Contract No. NASw 2035, by SCITRAN, P.O. Box 5456, Santa Barbara, California, 93108.